UNIVERSITY OF LJUBLJANA

Faculty of Mechanical Engineering

Performance study of different equivalent circuit topologies for modelling commercial Li-ion batteries

An undergraduate thesis of the first-cycle professional study programme in
MECHANICAL ENGINEERING

Álex Gandía Santaya

Ljubljana, June 2018

UNIVERSITY OF LJUBLJANA

Faculty of Mechanical Engineering

Performance study of different equivalent circuit topologies for modelling commercial Li-ion batteries

An undergraduate thesis of the first-cycle professional study programme in
MECHANICAL ENGINEERING

Álex Gandía Santaya

Advisor: Professor Tomaž Katrašnik

Ljubljana, June 2018

Acknowledgements

Declaration

1. I, the undersigned Álex Gandía Santaya, born 22 January 1996, a student at the Faculty of Mechanical Engineering at the University of Ljubljana, hereby declare that this undergraduate thesis titled *Performance study of different equivalent circuit topologies for modelling commercial Li-ion batteries* is my own original work created under the supervision of professor Tomaž Katrašnik.

2. I hereby declare that the submitted electronic copy of this undergraduate thesis is identical to the printed copy.

3. Pursuant to the provisions of the Copyright and Related Rights Act (Official Gazette of the Republic of Slovenia, No. 21/1995 as amended), I hereby expressly give my permission for this undergraduate thesis to be published on the websites of the Faculty of Mechanical Engineering and the University of Ljubljana.

4. By signing this Declaration, I grant my permission for this undergraduate thesis to be made publicly accessible online via the Repository of the University of Ljubljana.

By signing this document, I certify that:
- the presented text is the product of my own original research in its entirety;
- the presented text adheres to linguistic and stylistic conventions and the technical requirements of the Guidelines for Composing Final Theses, meaning that:
  - the works and opinions of other authors used in this undergraduate thesis are appropriately cited or acknowledged pursuant to the Guidelines for Composing Final Theses, and
  - I have obtained the permission for the use of any data and original work reproduced in the text in full (either as text or as a graphic) from their respective authors and duly noted that in the text itself;
- I am aware that plagiarism, i.e. the misrepresentation of someone else's work (be it text or graphics) as my own, is a crime under the Criminal Code of the Republic of Slovenia (Official Gazette of the Republic of Slovenia, No. 55/2008 as amended);
- I am aware of the potential repercussions concerning my status at the Faculty of Mechanical Engineering at the University of Ljubljana as per the applicable Rules should plagiarism be proven in connection to the submitted undergraduate thesis

Ljubljana, 6 June 2018   Signature of the author:_____

Abstract (in English)

Performance study of different equivalent circuit topologies for modelling commercial Li-ion batteries

In order to further promote use of electrified vehicles, a reduction of battery production costs and prolongation of their service file are required. This calls for application of high fidelity battery models in the development process of electrified vehicles and in the batteries' monitoring and control units.

In this work, three different equivalent circuit models (ECMs) based on RC circuits were constructed. Governing equations were analytically derived and numerically solved using fourth order Runge-Kutta method. After the initial parameterization and calibration of each model, comparison between simulated and experimental results obtained from commercial LI-ion battery measurements was performed. Additionally, a sensitivity analysis of the model parameters was performed in order to evaluate their contributions to end result.

Table of contents

List of figures

List of tables

List of symbols used

Symbol	Unit	Meaning
DoD	%	Depth of discharge
SoC(t0)	%	Initial state of charge
Q	Ah	Cell capacity
R_{int}	Ω	Internal resistance of the battery
Ri	Ω	Ith resistor of the ith RC circuit
C_i	F	Ith capacitor of the ith RC circuit
ω	rad/s	Angular frequency
σ	$Ω·s^{-1/2}$	Warburg coefficient
θ	$F·s^{n-1}$	CPE constant
SoC(t)	%	SoC time dependency

List of acronyms used

Acronym	Meaning
EVs	Electric vehicles
HEVs	Hybrid electric vehicles
EDVs	Electric-drive vehicles
ECMs	Equivalent circuit models
SoC	State of charge
SoH	State of health
EIS	Electrochemical impedance spectroscopy
OCV	Open-circuit voltage
DoD	Depth of discharge
AC	Alternating current
SEI	Solid-electrolyte interphase
BMS	Battery management system
DC	Direct current
KVL	Kirchhoff´s voltage law
KCL	Kirchhoff´s current law

1. Introduction

Nowadays, we're going through a change in the politics of energy. Renewable energy and electric cars are becoming competitive with technologies based on fossil fuels. However, for the new technologies to become the only alternative, we need to optimize existing battery technologies, so we can easily store energy efficiently with the minimum possible cost. Here is where electric batteries, especially lithium-ion battery cells, are playing an important role in society. In fact, lithium-ion batteries are being used in many different applications such as powering laptops, smartphones or in highly exigent performances such as electric vehicles (EVs), hybrid electric vehicles (HEVs) or electric-drive vehicles (EDVs).

To predict the behaviour of an electric battery, many different models have been proposed, which can be generally divided into three different categories: electrochemical models [1], equivalent circuit models (ECMs) [2] and empirical model [3].

Regarding electrochemical models the achieved accuracy is high, but the complexity of the model is also high and some complex parameters need to be calculated. Regarding ECMs, resistors, capacitors and voltage sources are used to represent underlying electrochemical and transport phenomena inside a battery cell in which each element of the circuit has a physical representation [4].

Compared to the electrochemical models, EC models are computationally less demanding and therefore real-time capable. On the other end, ECM models in general feature better trade-off between model complexity its prediction capability and ease of parametrization compared to the empirical models as topology and model parameters of ECM models can to some extend be related to particular phenomena in batteries, whereas in empirical models this interrelation in general less intuitive [4].

Batteries should not be overcharged or over-discharged to avoid damaging the battery, reducing the battery life and its performance, and causing even fire or explosions. So, the main goal of recent researches are system analysis, design, control and optimization of electric batteries.

Battery modelling has made important breakthroughs in recent years but when modelling an ECM, many things, such as the ambient temperature, the state of charge (SoC), the state of health (SoH), etc., must be considered to achieve an acceptable accuracy in the results.

The main goal of developing an ECM is to study the results under a lot of different situations by using computer simulation. This simulation should connect laboratory results to real-life measured data, so laboratory results may be used to predict battery performance in real life. The advantages of using ECMs are the simple model structure, low computational expense and acceptable accuracy. For these reasons, ECMs will be used for modelling the commercial Li-ion battery.

For battery analysis, a recent technique is being used lately. Electrochemical impedance spectroscopy (EIS) is a non-destructive technique that can provide time dependent information about the properties but also about ongoing electrochemical processes. Basically, this technique is used to determine the impedance of an electric battery in a very wide range of frequencies [5].

In this paper, ECMs are chosen to study the behaviour of a commercial Li-ion battery because they are simple, fast, robust, with a good compromise of accuracy/simplicity, and is easily integrated into simulation software. Three validations with three different ECMs, specifically the first, the second and the third order RC model, are going to be carried out. For validations of the models, experimental results from commercial Li-ion battery were used.

1.1. Objectives

The main goal of this Undergraduate Thesis is to implement models to simulate the behaviour of a commercial pouch cell Li-ion battery.

To reach the main goal of this thesis we are going to divide the thesis in the following specific objectives:
- Knowing the basic functioning principles of Li-ion batteries, as well as some of the most important parameters in the field of batteries and the most established different types of Li-ion cells.
- Knowing some of the most important electrochemical phenomena inside a Li-ion battery cell.
- Defining the concept of battery model and classifying the existing models according to the scope of application.
- Knowing the different ECMs of an electric battery and classifying them according to the complexity, from the simplest to the complex model.
- Analysis of governing equations of the different ECMs.
- Simulation of the selected ECMs.
- Interpretation of the obtained results.

1.2. Structure of the work

This thesis is divided into nine chapters:

Chapter 1: Thesis motivation, scope and objectives are discussed.

Chapter 2: A brief introduction to the world of Li-ion batteries and its functioning is presented.

Chapter 3: A literature review of battery modelling techniques and the criteria for selecting the model are presented.

Chapter 4: Procedures of obtaining ECM parameters are presented.

Chapter 5: The way of proceeding when simulating and the provided data are presented.

Chapter 6: The employed methodology for obtaining the results is explained.

Chapter 7: The obtained results are presented and explained.

Chapter 8: Conclusions are presented.

Chapter 9: Bibliography is presented.

2. Li-ion batteries

2.1. History

Lewis designed the first Li-ion battery in 1912 [6], but it was not until 1970 that not rechargeable batteries started to be commercialized. Ten years later, some tests were carried out with the first rechargeable lithium battery models in 1980 [7], although none of these were successful. Some years later, some investigations about batteries based on ions of lithium were realised, and finally in 1991, Sony commercialized the rechargeable Li-ion battery for the first time [8].

Currently, there are many applications that use Li-ion batteries. At the beginning, this kind of batteries were only used in small devices such as mobile phones, laptops or music players. Later, Li-ion batteries started to be used in the automotive industry, in military uses and even in spatial satellites. In this way, its high performance and reliability allow this technology to be applied in a very wide range of different sectors [9].

2.2. Basics of Li-ion batteries

Li-ion cell consists of a cathode (positive electrode) and an anode (negative electrode) which are in contact with an electrolyte containing lithium ions. The electrodes are separated from each other by a separator, typically microporous polymer membrane, which allows the exchange of lithium ions between the two electrodes but not electrons. Figure 2.1 depicts the basic functioning principles of a Li-ion battery cell.

When the cell is being charged, both electrodes are connected to an electric source. The electrons are forced to move to the anode. At the same time, Li ions are doing the same movement but throughout the electrolyte. With this movement of electrons, the cell has gained electrochemical energy because of the difference of potential between the two electrodes. On the other hand, when the cell is being discharged, electrons move from anode to the cathode through the external load to do the work and Li ions move from anode to the cathode in the electrolyte [10].
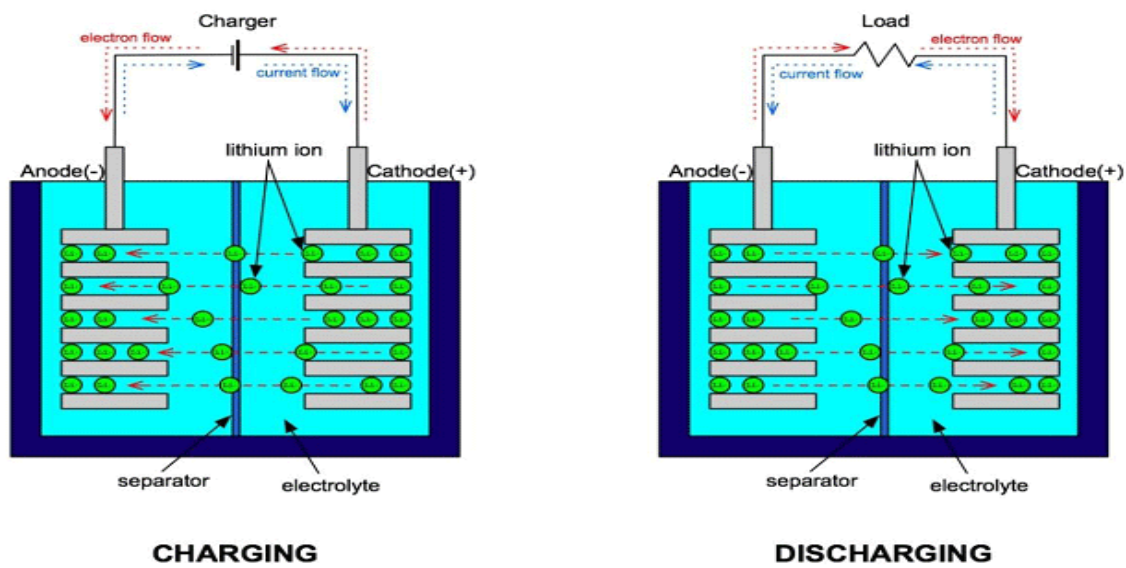
Figure 2.1: Functioning principles of a typical Li-ion battery cell subjected to charging and discharging processes respectively. Reprinted with permission of Meriam Sahin [11].

The performance of different types of batteries such as acid batteries, nickel metal hybrid batteries, Li-ion batteries, etc. may be compared by using the following parameters: specific energy, volumetric energy, specific capacity, cyclability, safety and the dis/charging rate. As we can see in Figure 2.2, Li-ion cells have the best performance regarding specific energy either by mass unit or volume unit and this is why they are being used for many different applications.
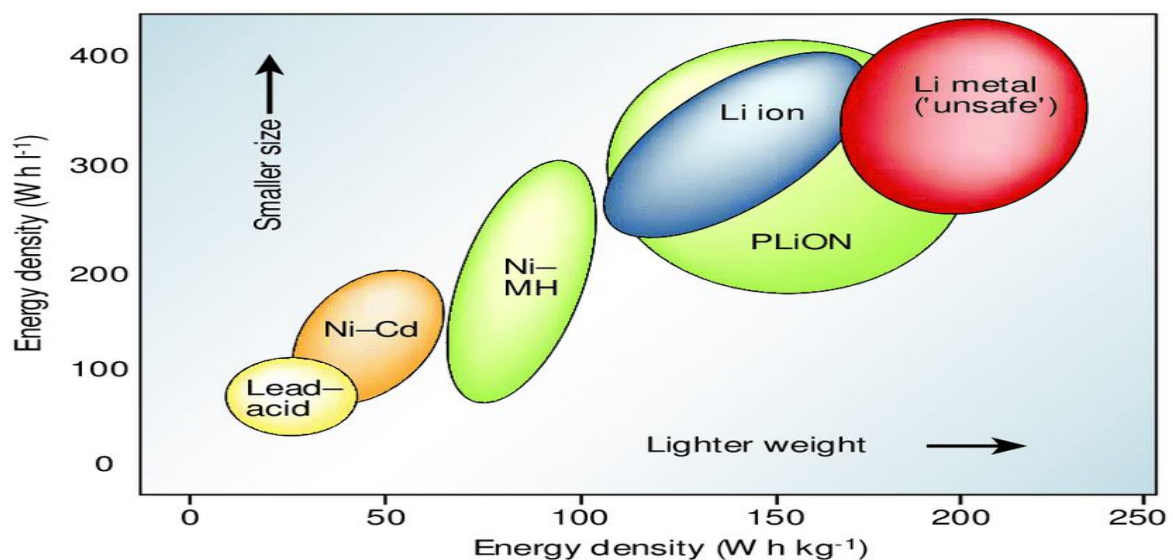
Figure 2.2: Comparison of energy densities of different rechargeable batteries. Reprinted with permission of Yan Wang [12].

2.2.1. Battery parameters

In this section, some of the most important parameters when describing the performance of an electric battery are going to be presented and explained.

- **State of Charge (SoC):** Available energy in a battery cell in a given moment. It is expressed with a percentage. For example, 100 % means the battery is fully charged and 0 % means that the battery is discharged.
- **Open-circuit voltage (OCV):** Terminal voltage of an electric battery when it is not being charged neither discharged. It is a function depending on the SoC of the battery as it is explained in Section 3.1.2. It is measured in volts (V).
- **State of Health (SoH):** It is a parameter that reflects the general condition of a battery and its ability to deliver the specified performance compared with a new battery. It is a measure of the long-term capability of the battery and gives an indication of how much of the lifetime energy has been consumed, and how much is left.
- **Depth of Discharge (DoD):** It is the complement of SoC:

$$DoD = 1 - SoC \ .$$
(2.1)

- **Specific energy:** It is a measure of the amount of energy per unit weight or per unit volume which may be stored in a battery. It may be measured in different units such as Wh/Kg, Wh/l, etc...
- **Cell capacity:** It is defined as the maximum draw of current during an hour that the battery can support. It is measured in Ah.
- **C-rate:** Charge and discharge rates are often denoted as C or C-rate, which is a measure of the rate at which a battery is charged or discharged relative to its capacity. It is measured with integer numbers followed by the letter C.

2.2.2. Typical materials of a Li-ion battery

Cathode materials of Li-ion batteries are compounds of lithium such as $LiFePO_4$, $LiCoO_2$, $LiMn_2O_4$, $LiNiO_2$, etc. Anode materials are usually Li_xC_6, TiS_2, V_2O_5, etc. The electrolyte is an organic solvent liquid, such as ethylene carbonate, propylene carbonate, dimethyl carbonate, etc., in which lithium salts are soluble, such as $LiPF_6$, $LiClO_4$, $LiBF_4$ [13]. Normally, separators are made of microporous materials, such as, polyethylene or propylene, which separate both electrodes, but allow the flow of ions.

2.2.3. Li-ion batteries performance

Nowadays, Li-ion batteries cover the biggest market share, ahead of the rest of batteries, being used for countless number of applications, especially those which need a high energy density [14]. In Table 2.1, some of the most important characteristics of these kinds of cells are shown.

Table 2.1: Advantages and disadvantages of Li-ion batteries in general [7].

Advantages	- High specific energy - Short charge times - Low internal resistance and high cell capacities (Ah) - Long lifetimes - Low self-discharge
Disadvantages	- Poor behaviour under cold temperatures (< 0 ℃) - Requires a protection system if the battery gets stressed - High degradation of the battery if it is exposed to high temperatures - There are several existing cases in which the battery exploded

2.2.4. Cell geometries

In this subsection, some of the most common Li-ion battery cells according its geometry are going to be presented. The growing demand of smaller cells has caused the development of different cells.

2.2.4.1. Cylindrical cell

Cylindrical cell (Figure 2.3) is the most widespread worldwide packaging style for primary and secondary cells. It is easy to manufacture and is mechanically stable and able to withstand increased pressure without suffering from deformation [15].
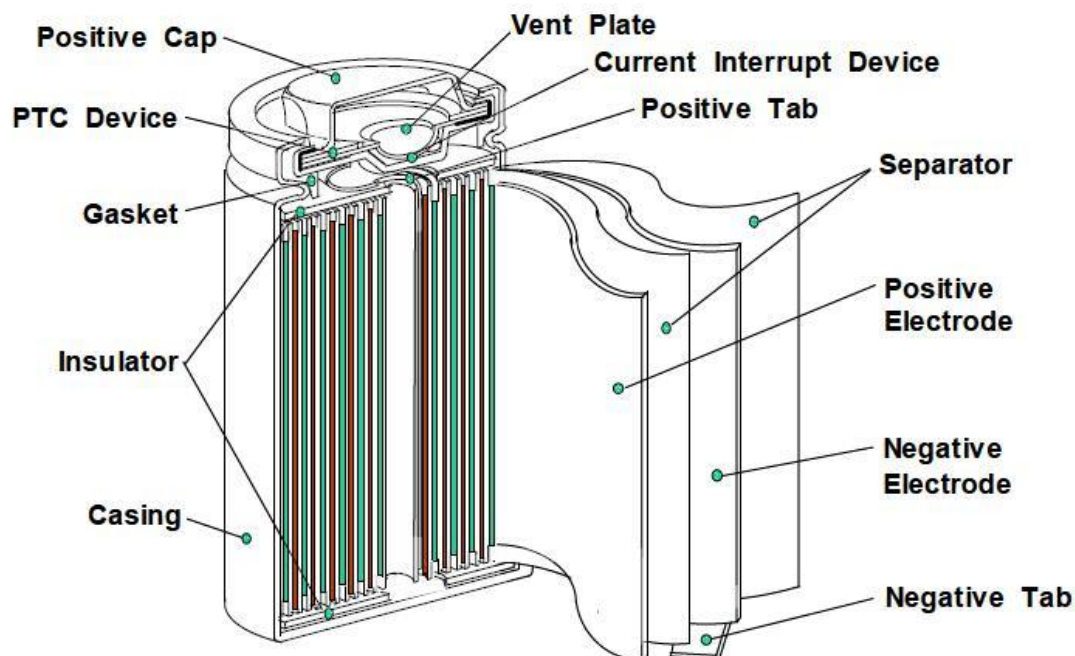
Figure 2.3: Scheme of the structure of a cylindrical Li-ion battery. Reprinted with permission of Global Tanpo [16].

2.2.4.2. Button cell

A compact design was built (Figure 2.4) to use in applications which required small battery cells such as watches, smart keys, sensors, etc. Nowadays, the most of these batteries are non-rechargeable [15].

Figure 2.4: Example of a button Li-ion battery cell [17].

2.2.4.3. Prismatic cell

Prismatic cell was introduced in the 1990s due to the demand for thinner size and lower manufacturing costs. These cells are mostly found in Li-ion mobile phone batteries [15].
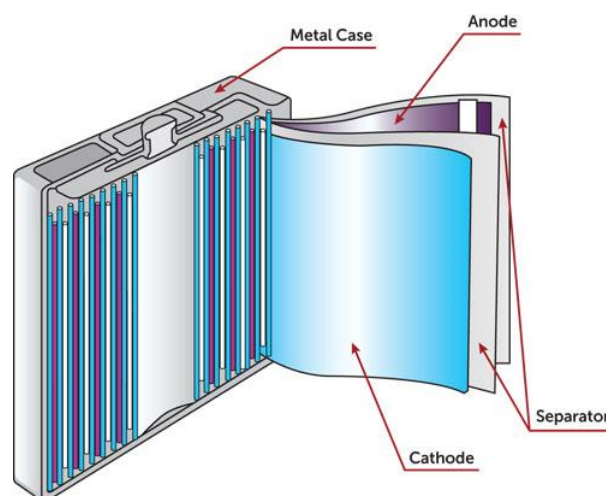
Figure 2.5: Scheme of the structure of a prismatic Li-ion battery. Reprinted with permission of Global Tanpo [18].

2.2.4.4. Pouch cell

The pouch cell (Figure 2.6) has the highest packaging efficiency among the rest of battery packs because of a laminated structure in a bag. These batteries are used in military and automotive applications. Notice that these cells do not have any standardization, so every manufacturer designs them by a tailor-made solution [15].

Figure 2.6: Example of a pouch Li-ion battery cell. Reprinted with permission of Targray [19].

2.2.5. Applications of the Li-ion batteries

Currently, Li-ion batteries are present in most of the daily activities. Depending on where we store a battery we can make the difference between these groups:
- Portable applications
- Industrial applications
- Automotive applications

Since 2004, the entire mobile phone batteries are based on Li-ion technology. This is a very important step since the market share of mobile phone batteries implies an 81 % of the all global market [20].

A rising in the use of electric batteries has been produced in industrial applications, due to the good performance of Li-ion batteries. These kinds of batteries are used in portable tools, or productive devices such as robots or variable renewal energy storage, etc. [21].

On the other hand, the sector which has experienced the biggest changes with the arrival of Li-ion batteries has been the automotive sector. Not long ago it was difficult to find a completely electric vehicle that could satisfy the demands of the consumer. Some attempts with lead-acid and NiMH had been done but without success [22].

Compared to other battery technologies, Li-ion batteries present the best features, especially energy density and specific energy, for being used in EVs.

2.3. Fundamentals of Li-ion battery dynamics

2.3.1. Electric and magnetic effects

Electric batteries are formed by cells connected to each other with wires, what leads to the presence of an inductance due to the wiring of the battery. This inductance is not very important in small cells as Li-ion cells and it is only remarkable at high frequencies (10-100 kHz).

Another phenomena that needs to be considered is called skin effect which appears when a high-frequency AC current is flowing through a material and because of the skin effect there is an extra resistance of the material to allow the current to flow through it. This resistance to let the current flow is measured with what is called current depth (mm) and tries to represent the part of the cross section that is being somehow covered to stop the flow of current, as we can see in Figure 2.7. As one would expect, the higher is the current depth, the higher would be the ohmic resistance of the battery. This skin effect determines the thickness of the current collector and the size of the electrodes when designing the cells. In Li-ion cells case, only at very high frequencies (10-100 kHz) this effect may influence the ohmic resistance of every cell and, consequently, the ohmic resistance of the battery [23].

Cross-sectional area of a round conductor available for conducting DC current

"DC resistance"

Cross-sectional area of the same conductor available for conducting low-frequency AC

"AC resistance"

Cross-sectional area of the same conductor available for conducting high-frequency AC

"AC resistance"
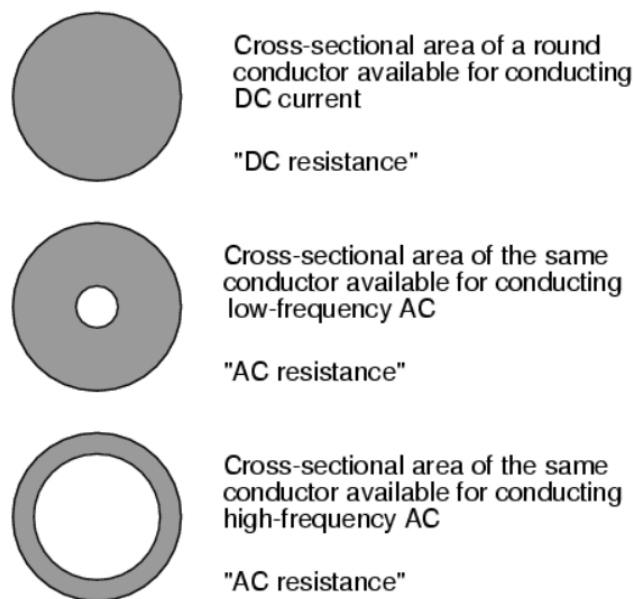
Figure 2.7: Skin effect depending on different current signals. Current depth increases as frequency increases. Reprinted with permission of All About Circuits [24].

2.3.2. Double-layer effects

The interface between the electrode and the electrolyte is the place where charge transfer takes place, and where electrochemical reactions are driven. Moreover, as a consequence of the short distance and the large surface of the electrode in contact with the electrolyte, a

charged zone is formed on the layer between the electrode and the electrolyte acting in a similar way to a capacitor, as we can see in Figure 2.8, and therefore this effect is called double-layer capacitance or electrochemical double layer [23].

$$C \propto \frac{A\uparrow\uparrow}{d\downarrow\downarrow}$$

A= 1000 or more m^2/g
d=Angstroms
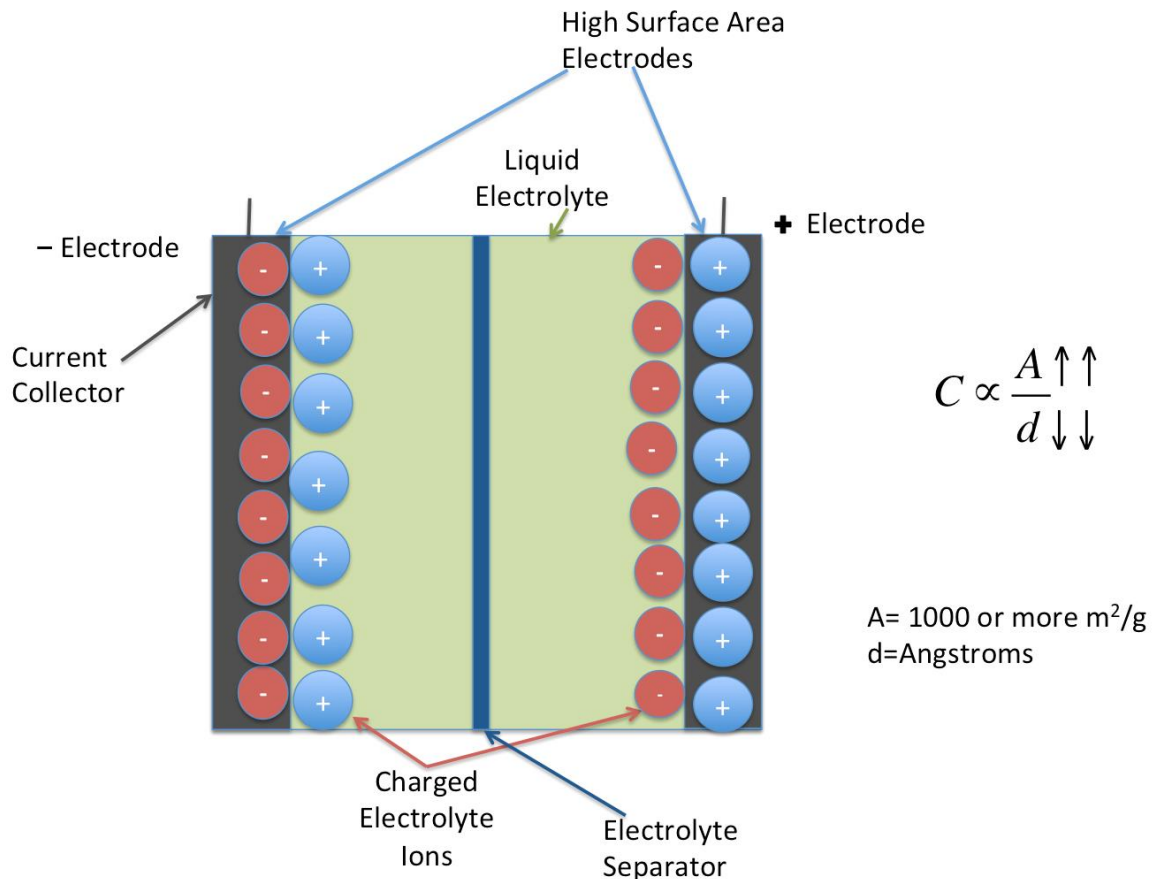
Figure 2.8: General scheme of the electrochemical double layer. Reprinted with permission of Marjan Aslani[25].

As we have already commented, in the interface between the electrode and the electrolyte takes place the electrochemical charge transfer reaction as well, and this is why the charge transfer reaction and the double-layer capacitance are modelled as a parallel network composed of a resistor R_{CT} and a capacitor C_{DL}. We need to bear in mind that both elements are not constant values, but dependent on different parameters of the battery as the SoC, the temperature or the current.

The current flow in this interface is very characteristic because a part of the current goes to the charge transfer reaction and another part goes to the double-layer capacitance, but as the capacitor only can store a limited amount of charge, it is mainly charged very quickly. After a short time, the whole current goes to the charge transfer reaction. When the battery is not under a charge pulse or a lower one, the capacitor is discharged and the whole current goes to the charge transfer reaction. In other words, the parallel network forms a low-pass filter for the charge transfer reaction and that is why double-layer capacitors only carry pulsating currents with high frequencies [23].

The value of the double-layer capacitance depends on many variables including electrode potential, temperature, ionic concentrations, types of ions, oxide layers, electrode roughness, etc [26].

2.3.3. Mass and electrons transport phenomena

Transport phenomena are those processes in which there is a net transference or transport of substance or energy. Regarding electric batteries, the transport of ions is done mainly by diffusion, which is a physical process in which a net movement of ions from a region of high concentration (or high chemical potential) to a region of low concentration (or low chemical potential) because of random motion of the ions happens [23]. In fact, diffusion can be found in different places inside the cell:

- The ions may be transported within the active mass to the porous electrode.
- In the porous electrode there is a movement of the ions to the electrolyte.
- In case of Li-ion batteries, there is a film, the solid electrolyte interface (SEI), on the surface of the anode. Diffusion of Li-ions through the SEI has a significant influence on the electric behaviour of Li-ion batteries.
- In the electrolyte or in the separator, since the ions may move from the anode to the cathode, and vice versa depending on whether the battery is being discharged or charged, respectively.

As every cell has two electrodes, both the active mass and the porous electrode diffusion phenomena have to be taken into account twice. At high frequencies, diffusing reactants do not have to move very far and that is why this effect is mainly important at low frequencies. At low frequencies the reactants have to diffuse farther, which affects the performance of the battery [23].

Regarding transport of electrons, the movement of the lithium ions creates free electrons in the anode which creates a charge at the positive current collector. The electrical current then flows from the current collector through a device being powered (cell phone, computer, etc.) to the negative current collector. The separator avoids the flow of electrons inside the battery [26].

2.3.4. Long-term effects

As its name indicates, now one of the most important long-term effects which take place under very low frequencies such as ageing effects is going to be explained. During a battery's lifetime, its performance tends to decrease because of chemical and physical processes that take place inside the cell with the continuous usage of the battery. Several processes may contribute to battery ageing, for example the electrolyte decomposition, the formation of SEI on both electrodes [27], the growth of dendrites [28], etc.

3. Battery modelling method

The arrival of the HEVs and the revival of the EVs have caused a growth in the research of the field of energy storage for this kind of vehicles. In consequence, it is important to have an efficient strategy when controlling the energy and a suitable mechanism of estimating the power level of the battery.

In order to reach an adequate control over the energy and the rest of important parameters of a Li-ion battery, numerous mathematical models that allow to simulate the behaviour of the battery and to predict future characteristics of the battery are being under investigation.

3.1. Ideal models

The battery is handled as a voltage source with unlimited power. These models are used if there is no interest in the performance of the battery.

3.1.1. The OCV model

We start with the simplest possible model. An ideal battery is modelled as an ideal constant voltage source, as we can observe in Figure 3.1.This model is inadequate and is only useful if the battery is unloaded and in complete equilibrium.
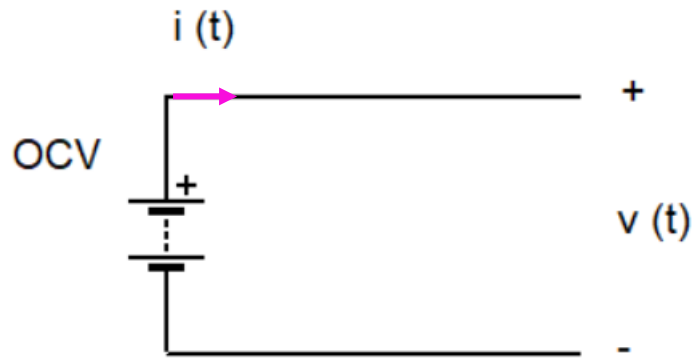
Figure 3.1: ECM of the OCV model

3.1.2. The OCV with SoC dependency

In this case, we also have an ideal voltage source, but the difference lies on the fact that there is a dependency of this ideal voltage source on the SoC.
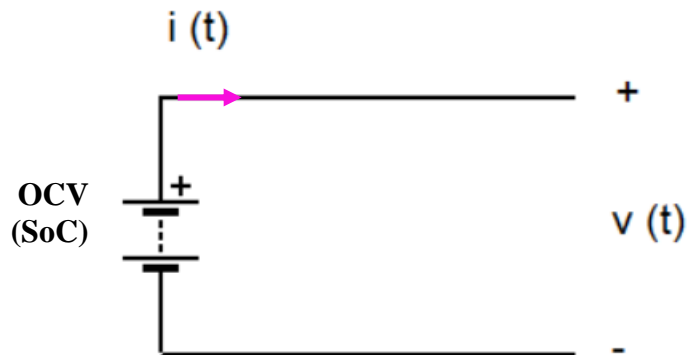
Figure 3.2: ECM of the OCV with SoC dependency model

We need to know the SoC time dependency to determine the value of OCV. There are many methods to estimate, and not to calculate, SoC [29]. In our simulated results we have chosen to use the Coulomb Counting method [30] which is one of the fastest and simplest ways.

Method integrates current over time, starting from an initial SoC and a known cell capacity in Ah. It is very important to know the signal current as we can see in equation (3.1):

$$SoC(t) = SoC(t0) + \frac{1}{Q} \int_{t0}^{t} Il(t)dt \quad . \tag{3.1}$$

Once we have the evolution of SoC throughout time, we can use this evolution to transform the SoC obtained data into terms of OCV by using an interpolation algorithm of a typical SoC vs OCV dependence, as we can see in Figure 3.3.

The example of Figure 3.3 represents the provided data by the manufacturer as it is explained in Section 5. When determining an OCV curve, the battery was discharged with low C-rates 10 % at a time. Then, the battery was rested a few hours and then the OCV was measured. This procedure was followed every 10 % low C-rate discharge and the shape of the final function was approximated by a polynomial function.
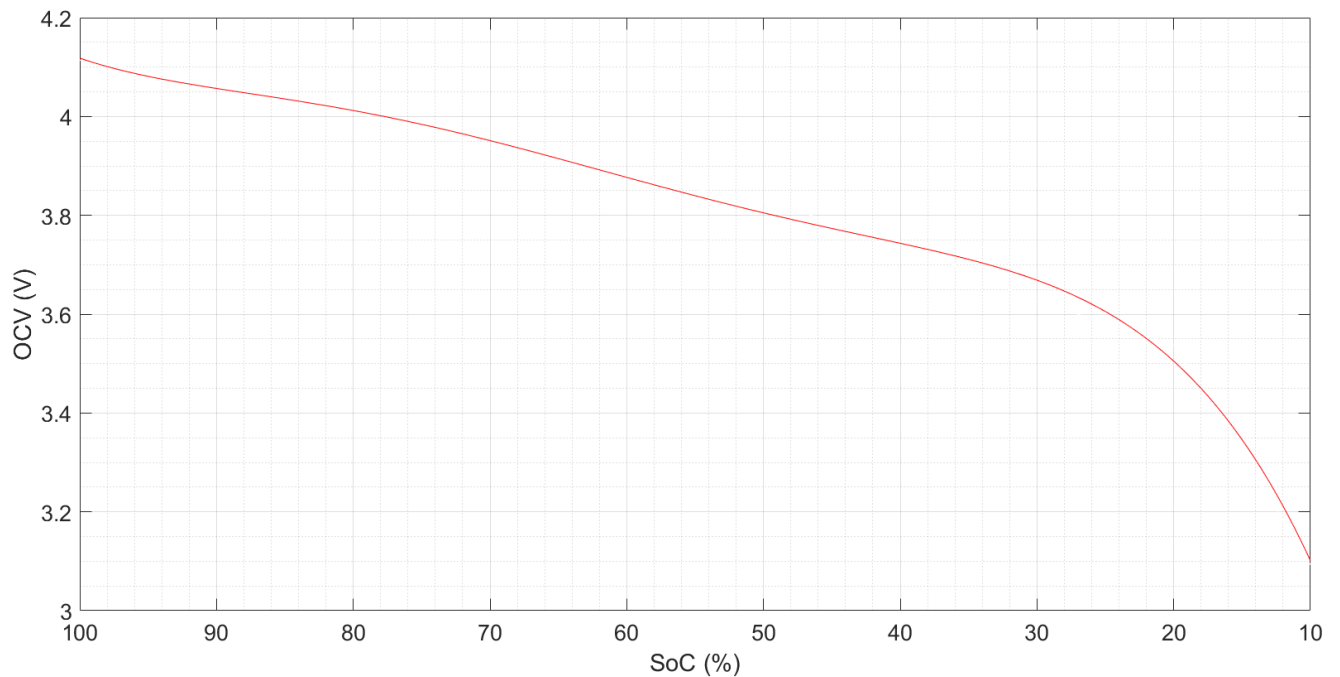
Figure 3.3: Example of a SoC dependent OCV for a typical Li-ion battery.

3.2. Equivalent circuit models

The equivalent circuit model (ECM) may be used to simulate the dynamic characteristics of the battery. It consists of circuit elements such as resistors, capacitors, a constant voltage source, etc. Thus, this model is widely used in various types of electric vehicle modelling simulations and battery management systems. In this section, some of the most important ECMs are going to be presented and analysed.

3.2.1. The Rint model

The Rint model, as shown in Figure 3.4, implements an ideal voltage source OCV to define the battery open-circuit voltage and a resistor R_{int} which is used to define the inner resistance of the battery. Both R_{int} and the OCV are dependent on SoC, the temperature and SoH [31].
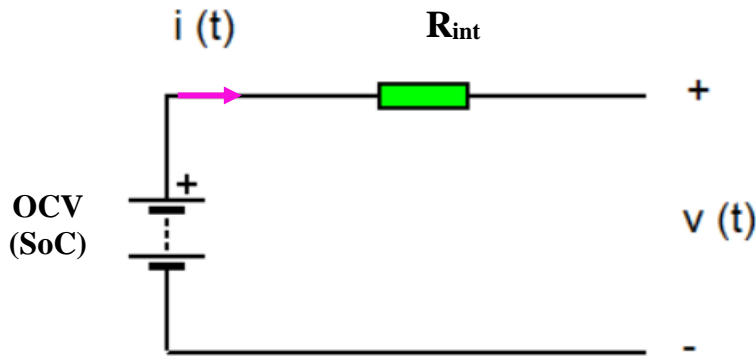
Figure 3.4: ECM of the Rint model

3.2.2. Obtaining of the system of differential equations

When modelling our ECMs we considered two passive elements (resistor and capacitor):

Resistor

A resistor is a passive two-terminal electrical component that implements electrical resistance as a circuit element [32]. In our models, there are different resistors that represent different electrochemical phenomena such as the internal resistance of the battery, the polarization resistance or the charge transfer resistance, for example.

The resistance is measured in Ohms (Ω). An Ohm is the resistance that occurs when a current of 1A passes through a resistor with a 1V drop across its terminals. The current is proportional to the voltage across the terminal ends. This ratio is represented by Ohm´s law:

$$R = \frac{V}{I} \quad . \tag{3.2}$$

Normally, in Li-ion battery ECMs the resistors which take part of the model are a variable value depending on the SoC, the temperature, the current and more variables, but as extensive measurement matrix should be performed to obtain dependencies, for our work we are going to deal with the resistors as constant values that can be approximated to these variable values.

Capacitor

A capacitor is a passive two-terminal electrical component that stores potential energy in an electric field. In our models, there are different capacitors that may represent different electrochemical phenomena such as the electrical double-layer of the battery or the polarization capacitance, for example.

Capacitance is defined as the ratio of the electric charge on each conductor to the potential difference between them. The unit of capacitance is the farad (F)

$$F = \frac{C}{V} \; ,$$
(3.3)

defined as one coulomb per volt.

Normally, in more accurate Li-ion battery ECMs, some kind of capacitors that present depression or correction factors, will be seen with Warburg and CPE elements in Section 4.1.2.3, are used. In this work, the capacitors are going to be treated as constant values to simplify the models.

The current that flows through a capacitor, *ic(t)*, may be written as

$$ic(t) = C \frac{duc(t)}{dt},$$
(3.4)

where C is the capacitance of the capacitor, $\frac{duc(t)}{dt}$ is the derivative of the voltage in the capacitor with respect to time.

As a demonstration of how we obtain the system of equations that provides the response of the terminal voltage of the battery in every case, we are going to deduce the system of differential equations for the first order RC model, respecting the nomenclature shown in Figure 3.5.

By using Kirchhoff´s voltage law (KVL) as

$$Uterm(t) = Ubat(SoC) + U0(t) + U1(t) \; ,$$
(3.5)

where *Ubat(SoC)* is a function depending on the SoC, *U0(t)* represents the voltage drop due to the inner resistance of the battery and *U1(t)* represents the voltage drop due to the dynamic phenomena of the battery, we get the terminal voltage response of the model, *Uterm(t)*. If we apply Ohm´s law in the voltage drop due to the inner resistance (U0) of the battery as

$$U0(t) = Rint * Il(t)$$
(3.6)

and then, we insert equation (3.6) into equation (3.5) we get

$$Uterm(t) = Ubat(SoC) + Rint * Il(t) + U1(t) \; ,$$
(3.7)

a new way of expressing the terminal voltage response of the battery. By using Kirchhoff´s current law (KCL) for node Y as

$$Il(t) = Ir(t) + Ic(t) \ , \tag{3.8}$$

where $Ir(t)$ is the current that flows through the resistor $R1$ and $Ic(t)$ is the current that flows through the capacitor $C1$. The sum of them represents the current flowing through the terminal of the battery, $Il(t)$. By using Ohm's law in $U1(t)$ as

$$Ir(t) = \frac{U1(t)}{R1} \ , \tag{3.9}$$

we get a new way of expressing $Ir(t)$.
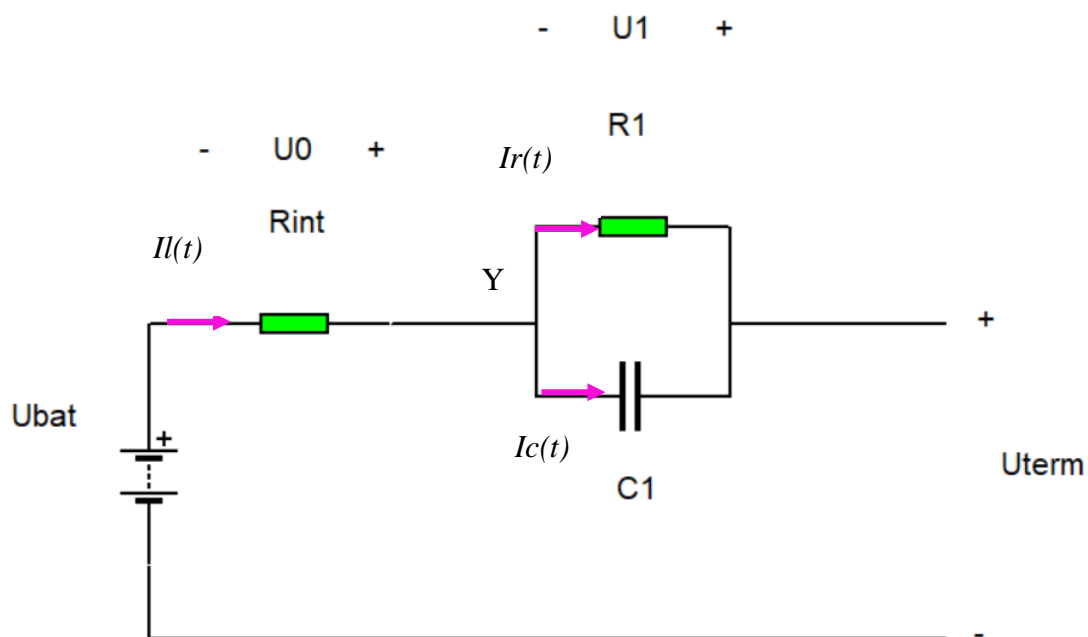
Figure 3.5: Scheme of the first order RC model

By definition, we know that

$$Ic(t) = C1 * \frac{dU1(t)}{dt} \ , \tag{3.10}$$

and putting equations (3.9) and (3.10) together into (3.8) as

$$Il(t) = \frac{U1(t)}{R1} + C1 * \frac{dU1(t)}{dt} \ , \tag{3.11}$$

we get a new way of expressing *Il(t)*. From simplifying equation (3.11) we get

$$\frac{dU1(t)}{dt} = -\frac{1}{R1 * C1} * U1(t) + \frac{1}{C1} * Il(t) \ , \tag{3.12}$$

that represents the time-dependent drop voltage across the RC circuit.

In order to take into account the dependency of the OCV on the SoC, we use the Coulomb Counting method as we already commented in Section 3.1.2.

Equations (3.12), (3.7) and (3.1) form the desired system of differential equations used for calculating the terminal voltage of the battery. The same procedure has been followed to get the systems of differential equations for the other RC models.

3.2.2.1. The first order RC model

The first order RC model consists of a resistor followed by a parallel RC circuit which is used to interpret the dynamics of the battery. The first order RC model is depicted in Figure 3.6. As we can see, there are four components: the open circuit voltage (OCV) which is a function depending on the SoC, the inner resistance R_{int}, the polarization resistance *R1* and the polarization capacitor *C1*. *U0* represents the voltage drop because of the inner resistance and *U1* represents the voltage drop because of the parallel RC circuit [31]. If we observe the terminal voltage of the battery, two cases may be distinguished:
- The battery is being discharged and is feeding a load. This event is represented by an impedance called load.
- The battery is being charged and is being fed by a charger. This event is represented by a DC voltage source.
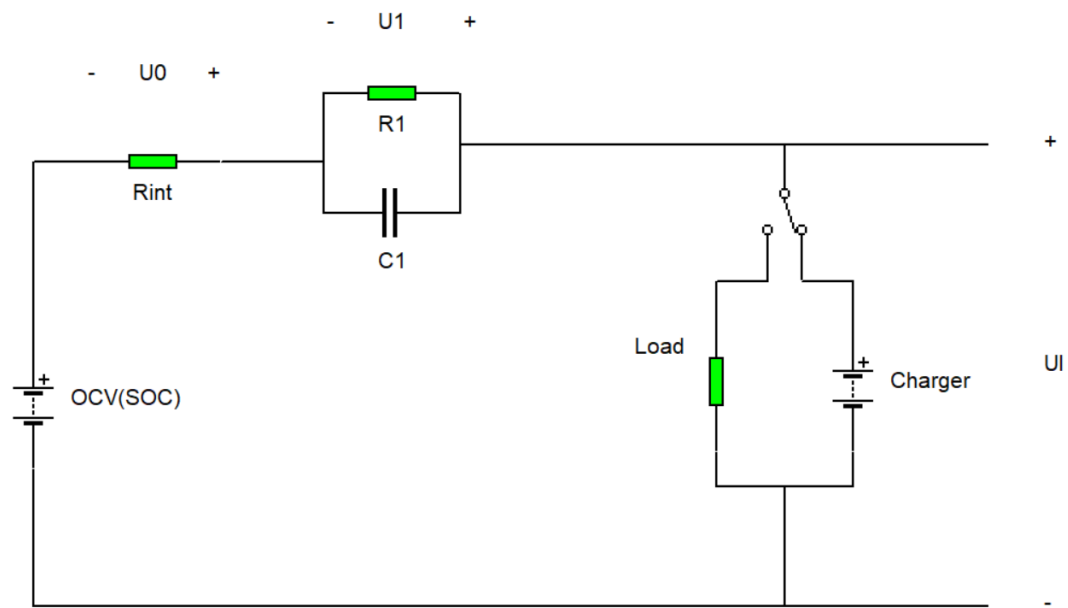
Figure 3.6: ECM of the first order RC model

From this ECM we obtain a system of equations (3.13) as

$$
\left\{
\begin{array}{l}
\dfrac{dU1(t)}{dt} = -\dfrac{1}{R1C1}U2(t) + \dfrac{1}{C1}Il(t) \ , \\[3ex]
SoC(t) = SoC(t0) + \dfrac{1}{Q}\displaystyle\int_{t0}^{t} Il(t)dt \ , \\[3ex]
Ul(t) = OCV(SoC) + U1(t) + Rint * Il(t) \ ,
\end{array}
\right.
\tag{3.13}
$$

which describes the terminal voltage response of the ECM under different inputs.

3.2.2.2. The second order RC model

The schematic diagram of the second order RC model is shown in Figure 3.7, where *OCV*, *Rint*, *R1*, *C1*, *U0*, and *U1* have the same meanings as in section 3.2.2.1, but there is an extra parallel RC circuit to describe the nonlinear polarization response of the lithium-ion battery. The resistance of the RC network, *R2*, is used to describe the concentration polarization, while the capacitance *C2* is used to describe the electrochemical polarization [31].

In regard to mathematical expressions, there is a system of equations

$$\left[\begin{array}{l} \dfrac{dU1(t)}{dt} = -\dfrac{1}{R1C1}U2(t) + \dfrac{1}{C1}Il(t) \ , \\[3em] \dfrac{dU2(t)}{dt} = -\dfrac{1}{R2C2}U2(t) + \dfrac{1}{C2}Il(t) \ , \\[3em] SoC(t) = SoC(t0) + \dfrac{1}{Q}\int_{t0}^{t} Il(t)dt \ , \\[2em] Ul(t) = OCV(SoC) + U1(t) + U2(t) + Rint * Il(t) \ , \end{array} \right. \qquad (3.14)$$

which describes the terminal voltage response of the ECM under different inputs.
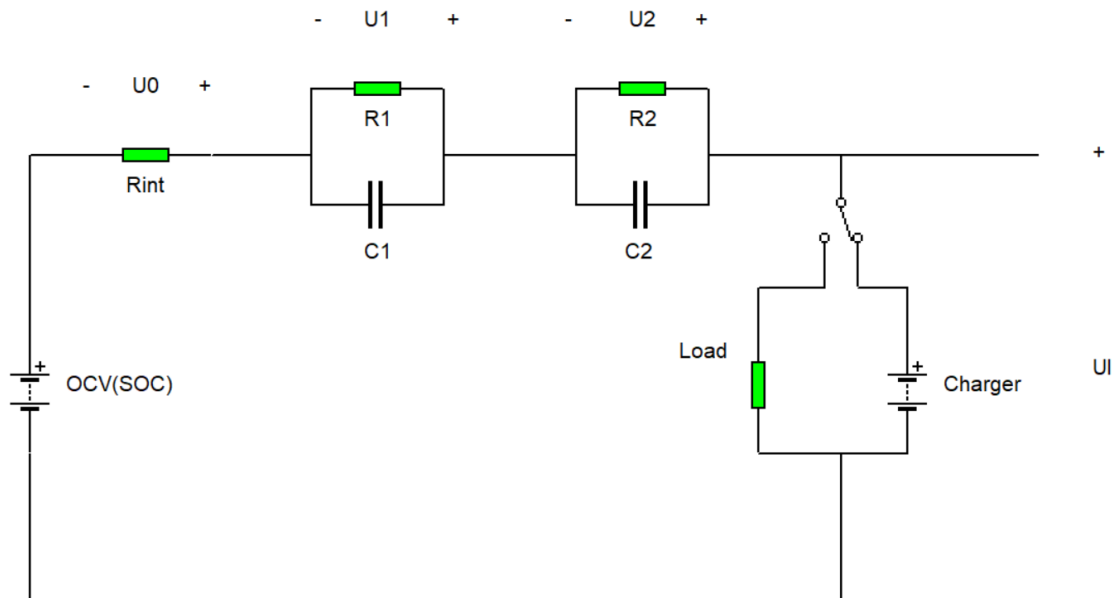
Figure 3.7: ECM of the second order RC model

3.2.2.3. The third order RC model

There are a lot of ECMs for the description of the battery behaviour. The first and the second order RC model are computationally simple, therefore these circuits are often used. However, if we want to get more accurate results, more RC circuits or more complicated components should be added to the ECM.

In this work, we have decided to add another RC circuit, since the complexity of the model is increased, but not excessively. If the tuning of parameters is carried out in a proper way, it is expected that results will be more accurate because the dynamic phenomena of the battery will be simulated in a more realistic way with the third order RC model (Figure 3.8).
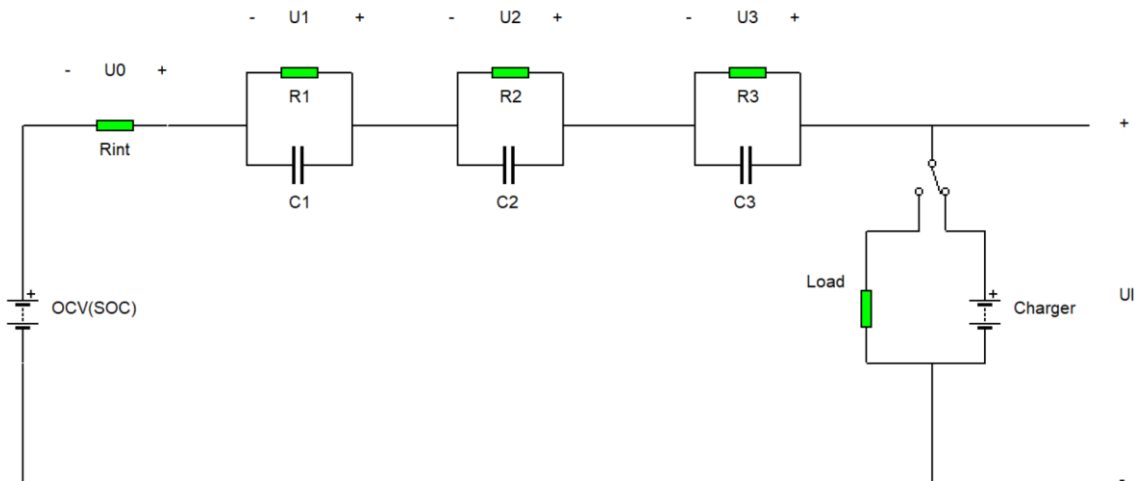
Figure 3.8: ECM of the third order RC model

From following the same procedure that was explained in Section 3.2.2 we get the following system of equations:

$$\frac{dU1(t)}{dt} = -\frac{1}{R1C1}U1(t) + \frac{1}{C1}Il(t)$$

$$\frac{dU2(t)}{dt} = -\frac{1}{R2C2}U2(t) + \frac{1}{C2}Il(t)$$

$$\frac{dU3(t)}{dt} = -\frac{1}{R3C3}U3(t) + \frac{1}{C3}Il(t) \tag{3.4}$$

$$SoC(t) = SoC(t0) + \frac{1}{Q}\int_{t0}^{t} Il(t)dt$$

$$Ul(t) = OCV(SoC) + U1(t) + U2(t) + U3(t) + Rint * Il(t)$$

3.3. Selection of the model

Throughout section 3, different Li-ion battery models have been presented. Some authors [33] have decided to simulate all these models and compare all of them with the same Li-ion real battery under identical conditions. Many of these results were very similar to the measured data.

Independent of the project, it is necessary to follow a series of criteria when choosing the model to use in the simulation. The criteria we need to keep in mind are the following ones:

- **Field of application.** It is necessary that the chosen model fits adequately to the field of application in which is going to be applied. In this work, electrochemical models and ECMs, which are mainly used in the field of automotive, have been

presented. Nevertheless, there will be investigations in which will be better to use one model or another.

- **Degree of accuracy.** This criterion is linked with the complexity of the model. It is important to define and set the needed degree of accuracy in the study before choosing the model, since usually higher accuracy means a higher complexity of the model. Exact models require more computational resources and time than simpler models, but they are valid for certain applications.
- **Degree of complexity.** It is important to take this parameter into account when choosing between several models. The complexity of a model may be influenced by the computer simulation, the determination of parameters of the model or the complexity of the governing equations.
- **Determination of parameters.** In some cases, obtaining of model parameters (R_{int}, R_1, C_1, etc.) is fairly simple by testing the real battery to simulate. In other cases, the deduction of these parameters is not that easy and very complicate mathematical calculations must be done, for example the techniques based on the recursive least square algorithm [34].
- **Calculation time.** It is important to determine how much time will be employed in calculations, since computational time is crucial in real-time applications. Complex simulations will take more time and computational cost.

4. Determining of parameters for ECMs

In section 3, many different models have been presented to simulate the behaviour of an electric battery. However, the parameters of these models (R_1, C_1, R_2, etc) are unknown initially and need to be determined.

For determining values of these parameters, there are different experimental techniques available. In the following subsections, some of the most used techniques for determining the value of the parameters of an ECM are going to be exposed.

4.1. Techniques in the frequency domain

The main techniques for determining the parameters of an ECM in the domain of frequency are the stationary frequency analysis and the electrochemical impedance spectroscopy. However, the stationary frequency analysis just deals with linear systems, and since batteries present strong non-linearity, this technique is not fairly useful.

4.1.1. Stationary frequency analysis

The technique is based on the development of a transfer function that connects the input to the output. From this function and using the current as an input and the voltage as an output, it is possible to determine the impedance of the battery [35].

However, by using this technique we cannot model the non-linear parts of the battery and hence we only can use this method to get an approximation of the results.

4.1.2. Electrochemical impedance spectroscopy (EIS)

The electrochemical impedance spectroscopy is an experimental method to characterize electrochemical systems and is considered as one of the most accurate methods. This technique is based on applying an external voltage over an electrochemical system within a wide range of frequencies to determine impedance of the electrochemical system [36].

Since the current signal and the applied voltage over the battery may be measured, with these data we are able to calculate the impedance of the battery allowing us to do a parameter estimation of the ECM which conform the cell and, we can develop different ECMs that have a concordance with the obtained spectrum of impedances obtained by the EIS experiment. Besides, this experiment can be performed under different temperatures, different SOCs, different C-rate, etc…

As it is well known, an impedance may be a real or a complex number with its corresponding real and imaginary part. Nyquist, Bode and even a 3D plot can be used to represent a complex number under different frequencies. In this work, data will be represented by using Nyquist plot [36].

The shape of the curve is important in making qualitative interpretations of the data. The disadvantage of the Nyquist representation is that loses the frequency dimension of the data. One way of overcoming this problem is by labelling the frequencies on the curve.

EIS utilizes a small amplitude AC signal for determining the impedance characteristics of a cell. Notice that the parametrisation extracted from testing the battery with EIS will be applicable when the obtained ECM tries to predict the behaviour of the cell when small currents are demanded. Nevertheless, this parametrisation will have limited applicability when the ECM will be later used to model the behaviour of the cell under larger current demands such as drive cycles [37].

In order to overcome the above drawback, reference [38] propose superimposing the DC current offset over the EIS signals to determine the current dependency of impedance parameters. However, since significant time is required for the EIS test, the battery SoC changes significantly during the test procedure if the amplitude of the superimposed current is improper. This can lead to a lower accuracy of the parametrisation and make this method practically not applicable at moderate and high current rates [37].

In the following subsections, some different ECMs are going to be presented with corresponding Nyquist plots so we can understand how the EIS works and its relationship with electrochemistry. According to Nyquist plots we will be able to identify every single component of the ECM because its behaviour in the Nyquist plot. In this section, we calculated frequency response with different parameters. The complexity of the plots increases from the simple first RC model to an ECM including Zarc and Warburg elements.

4.1.2.1. EIS curve of a first order RC model

The aspect of a Nyquist plot of a first RC order model ECM is a semicircle shifted slightly to the right in the real axis as we can see in Figure 4.1. In order to see the influence of the parameters, two ECMs have been represented. We can see that:

- In both ECMs, R_{int} has the same value of 20 Ω since we can see both start from the same point.
- The only difference between two plots is the value of R_1. In the blue graphic, R_1 has a value of 250 Ω, as opposed to the red one, in which R_1 has a value of 150 Ω.

The semicircles are the result of a RC parallel network between R_1 and a capacitor which has a value of 40 µF in both cases.
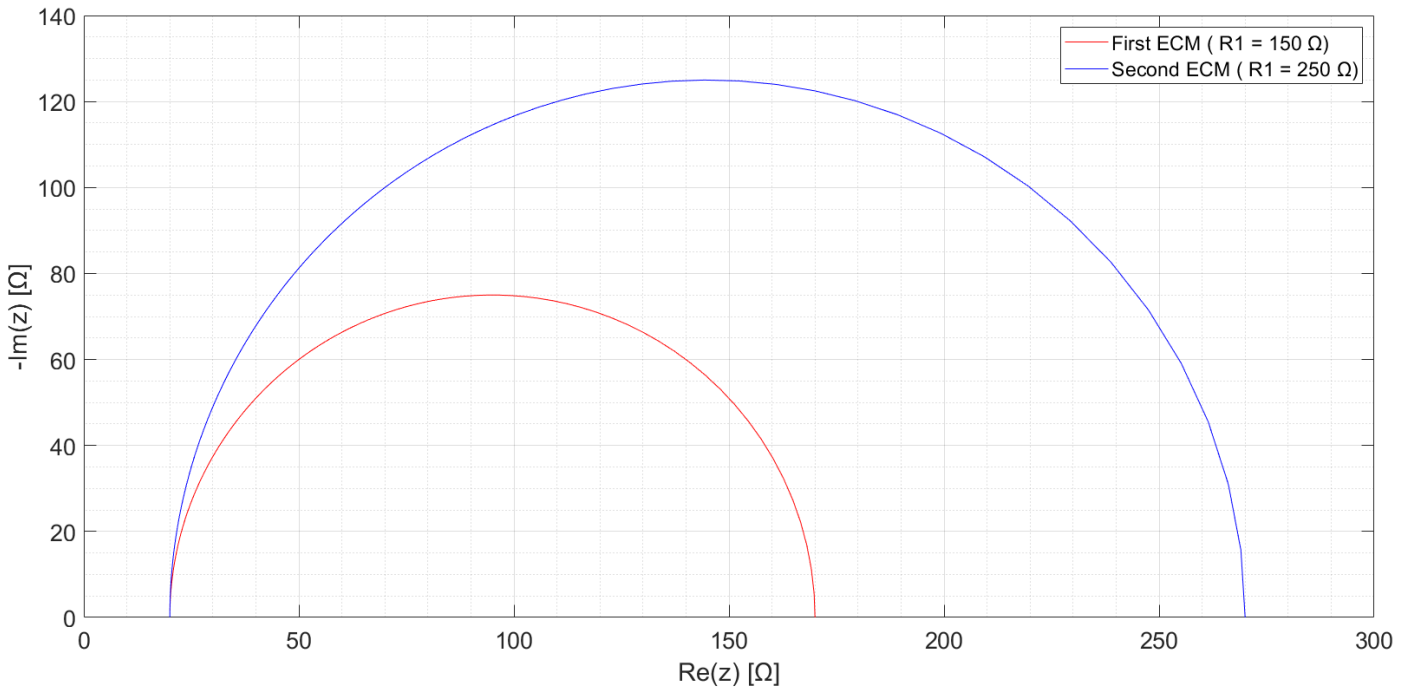
Figure 4.1: Nyquist plot of first order RC models with different parameters

The graphics in Figure 4.1 is obtained from solving the impedance function in the complex plane of a first order RC model with general parameters as we can see in equation (4.1):

$$Z = Rint + \frac{1}{R1(\frac{1}{R1^2}+C1^2\omega^2)} - \frac{iC1\omega}{\frac{1}{R1^2}+C1^2\omega^2} \qquad (4.1)$$

4.1.2.2. EIS curve of a second order RC model

The aspect of a Nyquist plot of a second RC order model ECM is a semicircle which is not finished followed by a straight line with a constant slope as we can see in Figure 4.2. Selected parameters have been the following ones:

- $R_{int} = 25\ \Omega$
- $R_1 = 250\ \Omega$
- $R_2 = 750\ \Omega$
- $C_1 = 40\ \mu F$
- $C_2 = 500\ \mu F$

In the low-frequency region (20-1 Hz), impedance spectroscopy looks like a straight line with a constant slope, a typical phenomenon of diffusion. In the middle-frequency region (33000-20 Hz), the impedance spectroscopy is a depressed semicircle caused by the charge transfer reaction at the electrode surfaces. In the high-frequency section (100-33 kHz), the

impedance spectra intersect with the real axis. According to what it has been already explained, this point could be explained by an ohmic resistance in the equivalent circuit.
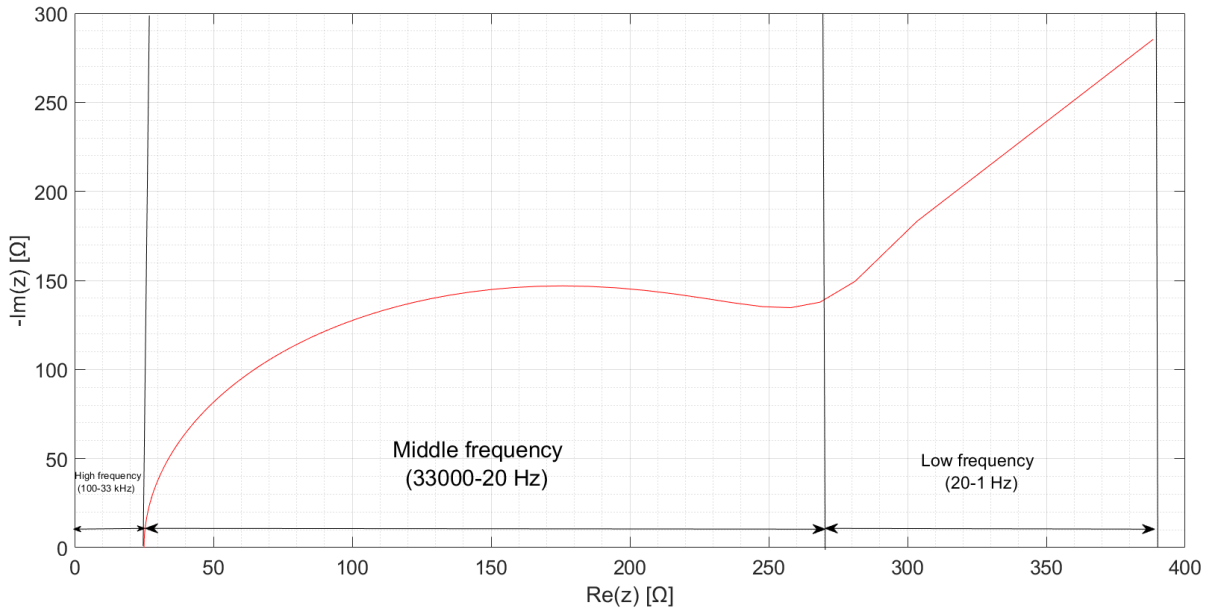

Figure 4.2: Nyquist plot of a second order RC model

The graphic in model is obtained from solving the impedance in the complex plane of a second order RC model with general parameters as we can see in the following equations (4.2) :

$$Re(Z) = Rint + \frac{1}{R1(\frac{1}{R1^2}+C1^2\omega^2)} + \frac{1}{R2(\frac{1}{R2^2}+C2^2\omega^2)}$$

$$Im(Z) = -\left(\frac{C1\omega}{\frac{1}{R1^2}+C1^2\omega^2} + \frac{C2\omega}{\frac{1}{R2^2}+C2^2\omega^2}\right)$$

$$(4.2)$$

4.1.2.3. EIS curve of an ECM with Warburg and Zarc elements

Warburg impedance: Part of the impedance called Warburg impedance is a consequence of diffusion effects. The impedance depends on the frequency of the potential perturbation. At high frequencies, the Warburg impedance is small since diffusing reactants don't have to move very far. At low frequencies, the reactants have to diffuse further, increasing the Warburg-impedance [40].
General expression of the impedance of a Warburg element may be modelled as

$$Zw = \frac{\sigma}{\omega^{\frac{1}{2}}} - i\frac{\sigma}{\omega^{\frac{1}{2}}} \; , \tag{4.3}$$

where σ is the Warburg coefficient and ω the angular frequency [41]. In Figure 4.4 we can see a Warburg impedance taking part of the ECM, denoted as *Zw*.

Zarc impedance: Zarc elements are a parallel connection of a resistor *R* and a constant-phase-element (CPE) which mathematical expression may be modelled as

$$Zcpe = \frac{1}{\theta(i\omega)^{\varphi}} \; , \tag{4.4}$$

where θ is a constant and φ is a coefficient which goes from 1 to 0. When $\varphi=0$, the CPE behaves as a resistor and when $\varphi=1$ the CPE behaves as a capacitor [41].

In his textbook, Macdonald [36] points out that even though a particular theory may not give exactly constant-phase-element CPE behavior, very often CPE behavior will fit experimental data so well that the deviations are totally masked by experimental noise and uncertainties. This is increasingly true as the complexity of a circuit model grows. In short, a CPE can provide a useful modelling element, even if the true nature of the system is unknown [41].

So far CPE has been identified with different physical phenomena such as the electrode roughness, inhomogeneous reaction rates on a surface, the varying thickness or composition of a coating [42].

The aspect of a Nyquist plot of an ECM with Zarc and Warburg element may be seen in Figure 4.3. There are two semicircles due to the Zarc elements, and there is also a linear slope with a determined angle due to a Warburg element that tries to represent the effects of diffusion outside the electrodes. The corresponding ECM may be seen in Figure 4.4 [43].
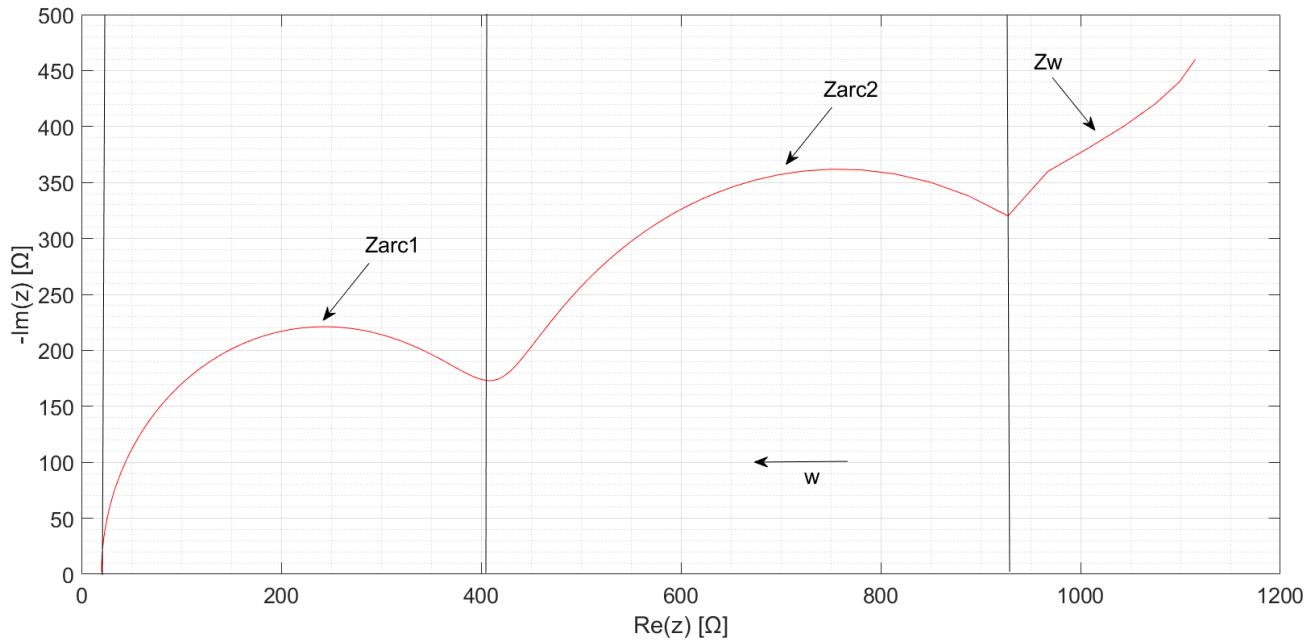
Figure 4.3: Nyquist plot of an ECM with Zarc and Warburg elements
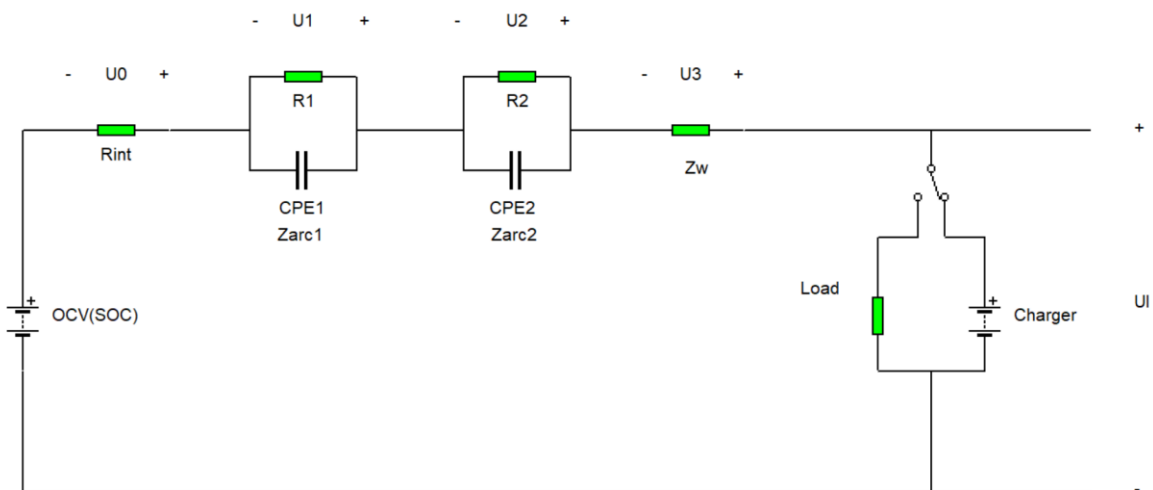
Figure 4.4: ECM with Zarc and Warburg elements

The graphic in Figure 4.3 is obtained from solving the impedance in the complex plane of an ECM as in Figure 4.4, but because of its complexity the previous ECM may be represented by an EC with three RC elements and its ohmic resistance, as we can see in equations (4.5):

$$
Re(Z) = Rint + \frac{1}{R1\left(\frac{1}{R1^2}+C1^2\omega^2\right)} + \frac{1}{R2\left(\frac{1}{R2^2}+C2^2\omega^2\right)} + \frac{1}{R3\left(\frac{1}{R3^2}+C3^2\omega^2\right)}
$$

$$
Im(Z) = -\left(\frac{C1\omega}{\frac{1}{R1^2}+C1^2\omega^2} + \frac{C2\omega}{\frac{1}{R2^2}+C2^2\omega^2} + \frac{C3\omega}{\frac{1}{R3^2}+C3^2\omega^2}\right)
$$

(4.5)

5. Simulation

Li-ion batteries are very non-linear in their behaviour, so it is very important that we know their dynamic response. We want to create an ECM that it is parameterised in such a way that the model respond behaves similar to the real battery.

Once the input data measured in real battery have been implemented in the model, we can move on to the computer simulation. When we have got the simulated results, we can compare them to the ones obtained in the experiment. Now, we can have two possible situations:

- **The deviation obtained during the simulation is acceptable.** The ECM may be implemented for predicting and controlling the behaviour of the battery in real life applications.
- **The deviation obtained during the simulation is unacceptable.** The loop works as an iteration time till we reach an acceptable deviation. Normally, this happens when the parameters have not been selected properly.

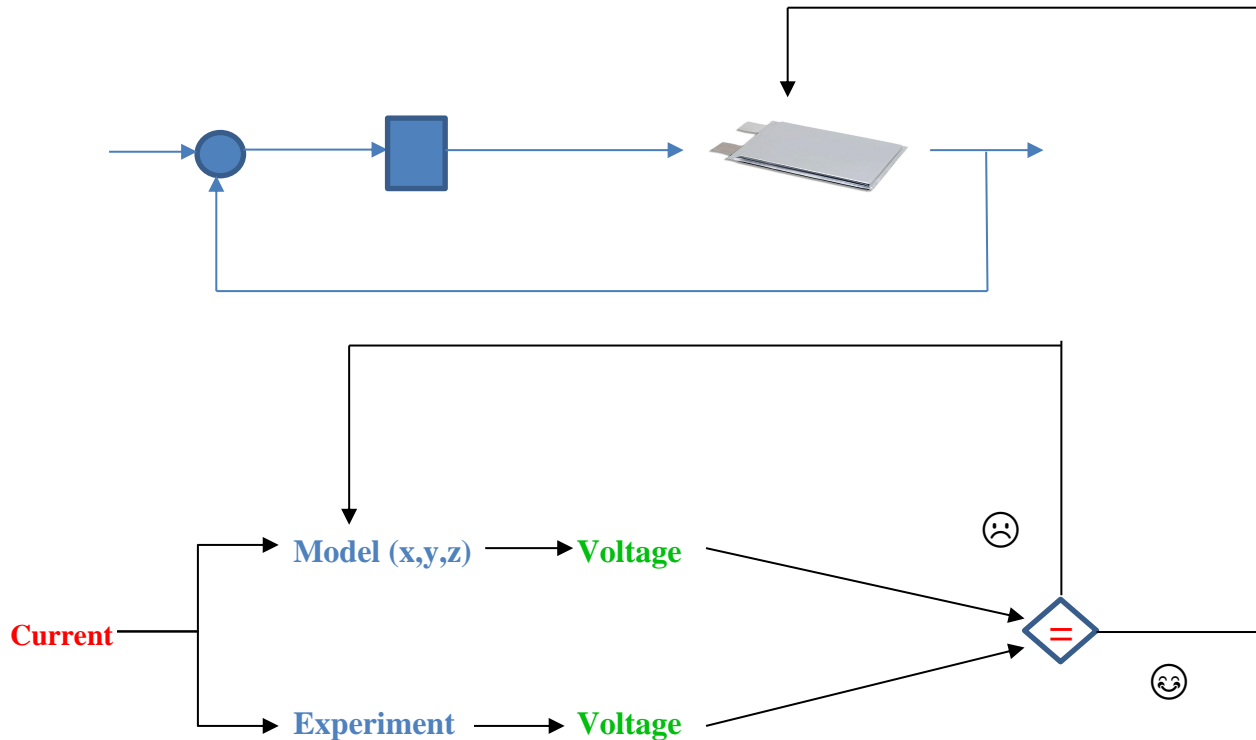A scheme of the parametrisation is represented in Figure 5.1:

Figure 5.1: Scheme of parametrisation of EC model.

In this work, we have decided to create three ECMs for a Li-ion battery whose characteristics are represented in Table 5.1. These ECMs were simulated under two different scenarios, so we could validate our models in a broader range of situations.

Table 5.1: Characteristics of the measured battery obtained from manufacturers datasheet.

Type of cell	Li-ion pouch cell	
Chemistry	Mn/NMC cathode	Carbon/Graphite anode
Capacity	41 Ah	
Internal resistance	0.7 mΩ	
Voltage range	3.0 to 4.15 V	
Weight	965 g	
Energy density	159 Wh/Kg	

In this work, we have been provided with some basic data extracted from two different experiments:

- **Pulse experiment.** In this experiment, generic current pulses have been applied to the battery obtaining time dependent terminal voltage response of the battery.
- **Dynamic experiment.** In this experiment, dynamic current pulses have been applied to the battery obtaining time dependent terminal voltage response of the battery [44].

In order to consider the OCV dependency on SoC, we have been provided with measurements that are presented in Figure 3.3.

Besides, some additional data have been provided with the EIS method of the battery under different SoCs (from 10 % to 100 %). Real and the imaginary part of a complex number in a certain frequency were measured, so we can generate a Nyquist plot depending on the SoC of the battery we want to analyse.

6. Methodology

This chapter explains and justifies the methods and processes used for obtaining measurements, calculations and modelling procedures.

6.1. Using the computer programs for the simulation

In this work, computer programs such as MATLAB, Dev-C++, Wolfram Mathematica, Microsoft Excel and Code: Blocks have been used in the elaboration and the obtaining of the results.

Dev-C++ and Code: Blocks, were used for programming in C and C++ language. In our work, these programs have played a very important role since they have been used for solving the system of differential equations of every case. The method used for solving these systems of differential equations has been 4th order Runge Kutta method.
Wolfram Mathematica was used for simplifying mathematical expressions, especially when operating with complex numbers for representing Nyquist plot.

Microsoft Excel was mainly used for working with .txt files since the provided data have been stored in this format.

6.2. Determination of the parameters for the model

In this work, parameters were treated as constant values. If the parameters would have been treated as dependant functions of temperature and SoC a higher accuracy would have been obtained.

Initial values of different parameters that have been used in the simulation of our models are based on [45]. After initial simulation we have tried to tune these parameters by observing and comparing voltage response between simulated and experimental data.

Specifically, we have selected a sample of the pulse experiment in where discharging current pulses and its corresponding terminal voltage response have been zoomed in, as we can see in Figure 6.1. Starting from initial values based on [45], parameters have been tuned in a

way that the simulated voltage response looks as similar to experimental voltage response as possible.
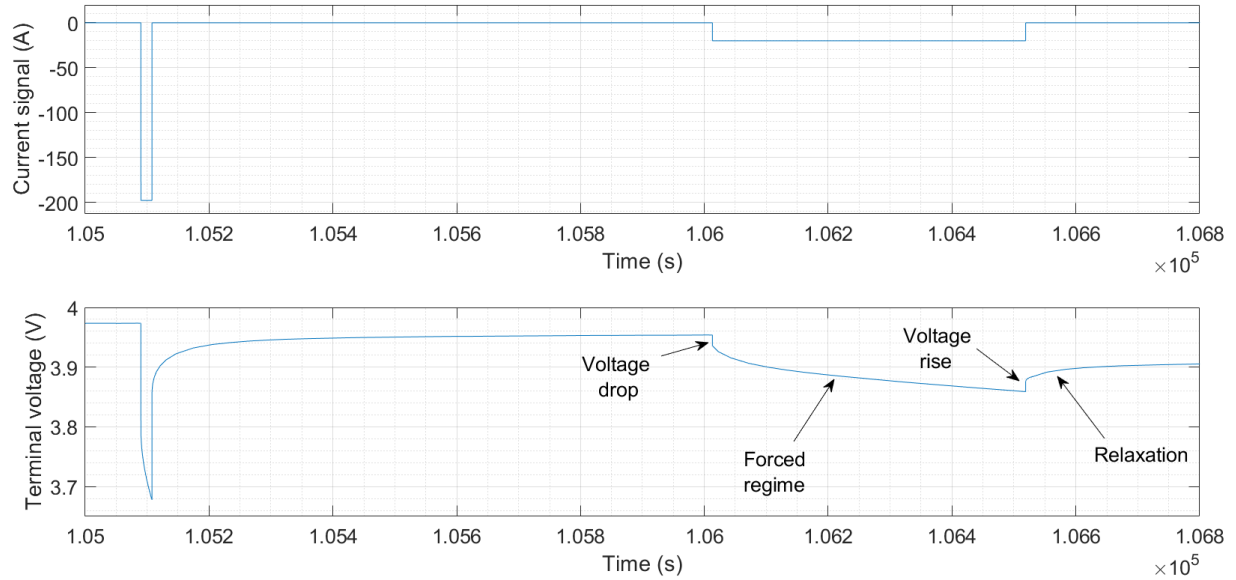

Figure 6.1: Sample of the signal current and the experimental voltage response selected for determining the parameters of the models.

7. Results and discussion

This section presents the results obtained from simulating the first, second and third order RC models. Simulations have been carried out under two different load profiles as it was already commented in Section 5.

First of all, we are going to show the two different currents that have been applied over the battery for testing the response of the terminal voltage of the battery under different scenarios.

As we can see in Figure 7.1, the battery has been tested under high discharging and charging currents (up to 5C rate) within short periods of time (dynamic experiment), so we can see the behaviour of the battery under wide variety of loads.
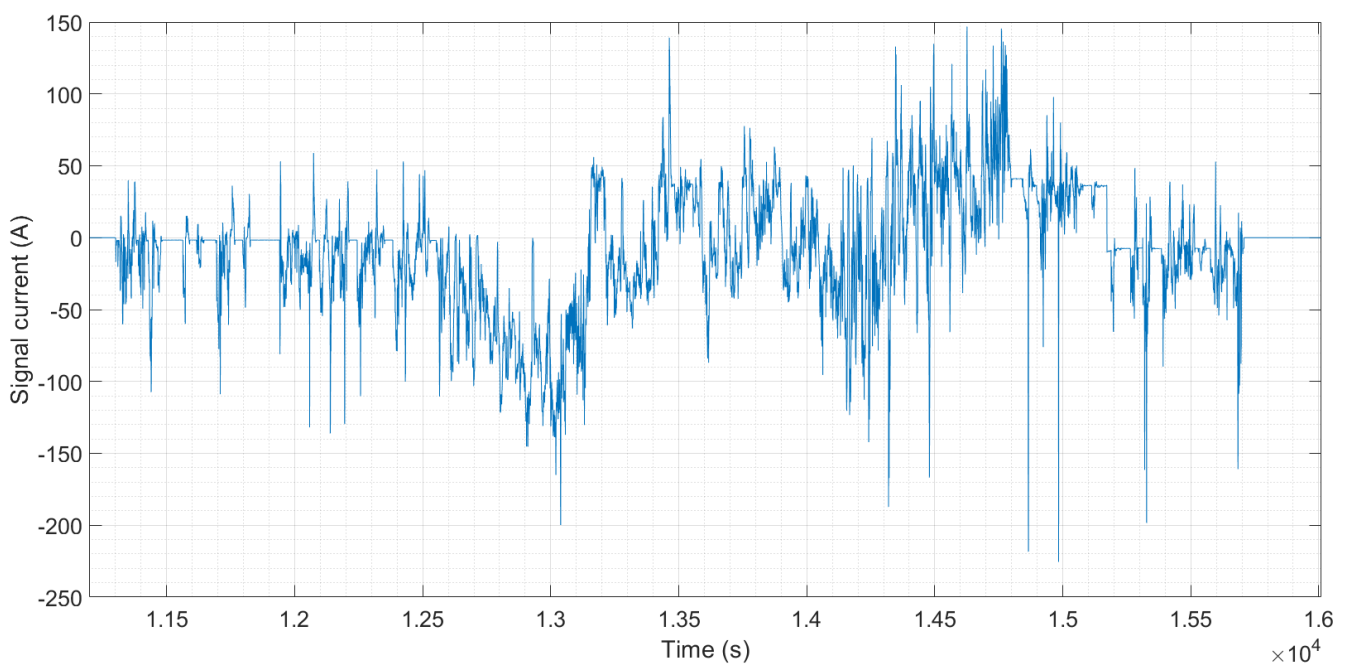

Figure 7.1: Current signal applied over the battery in the dynamic experiment

Figure 7.2 represents periodical discharging and charging peaks of current (pulse experiment), so we can see the behaviour of the battery under periodical functioning.
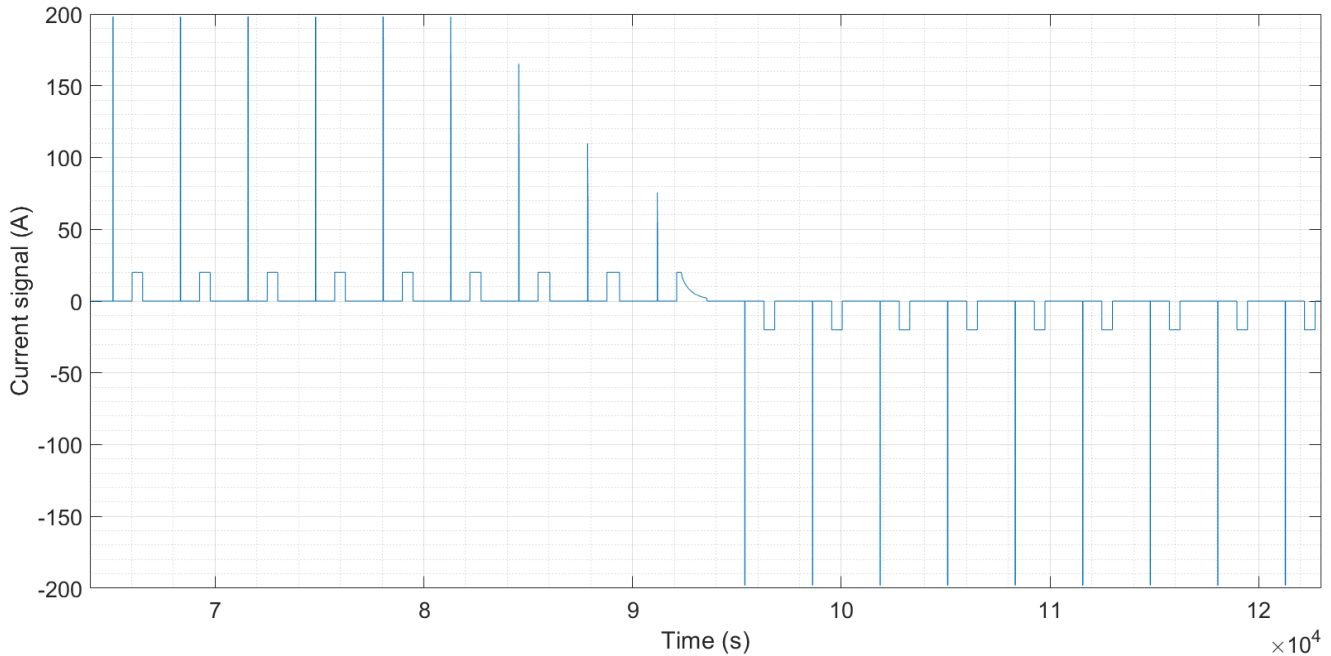

Figure 7.2: Current signal applied over the battery in the pulse experiment

For determining the initial SoC when testing the battery, since we had the initial experimental terminal voltage of the battery and we also had the data provided in Figure 3.3, we did an interpolation by hand for determining the initial state of charge.

After the end of a charging or a discharging pulse, the battery voltage approaches new steady state, if no current is being applied to the battery. This corresponds to battery relaxation and this behaviour of the battery is related to phenomena inside itself such as polarization and mass transfer (2.3.3). These phenomena have slow response dynamics, causing voltage variations [46]. For example, the selected sample for determining the parameters of the models (Figure 6.1) shows the typical response of a battery following a discharge current pulse. The voltage measured at the end of the relaxation phase may be considered as the OCV of the battery at a given SoC, if the rest time is sufficiently long and there is no current applied anymore.

Figure 6.1 also shows two other phases of the battery response. These two phases are the voltage drop and the forced regime phase. The voltage drop is the consequence of a sudden change in the current level and is mainly influenced by the internal resistance of the battery. The forced regime phase appears in the response of the battery almost immediately after the sudden change in the current level.

After this brief explanation of the response of the battery, the results for every model are going to be presented and discussed in the next subsections. Additionally, in the next subsections, we are going to use the next nomenclature for referring to the different models:

- First order RC model is going to be referred-to as 1RC model.
- Second order RC model is going to be referred-to as 2RC model.
- Third order RC model is going to be referred-to as 3RC model.

7.1. Simulation results for 1RC model

It should be expected that if the tuning of parameters has been properly done, this ECM should be the less accurate between the three of them. In other words, the mean relative deviation between the simulated data and the experimental data should be the highest. Obviously, this is because 2RC and 3RC models have a capability to describe the non-linear polarization response with two or three RC circuits instead of just one RC circuit compared to 1RC model.

7.1.1. Tuning of parameters

The result of tuning the parameters for 1RC model is shown in Figure 7.3. Note that the simulated data fit better for the lower discharging current (0.5C rate) than for the higher discharging current (5C rate) because 1RC circuit does not feature all necessary frequency responses of the underlying phenomena inside the battery cell.

We can see that the output of the model is faster than the measured data in the relaxation voltage phase and the same may be said about the forced regime.
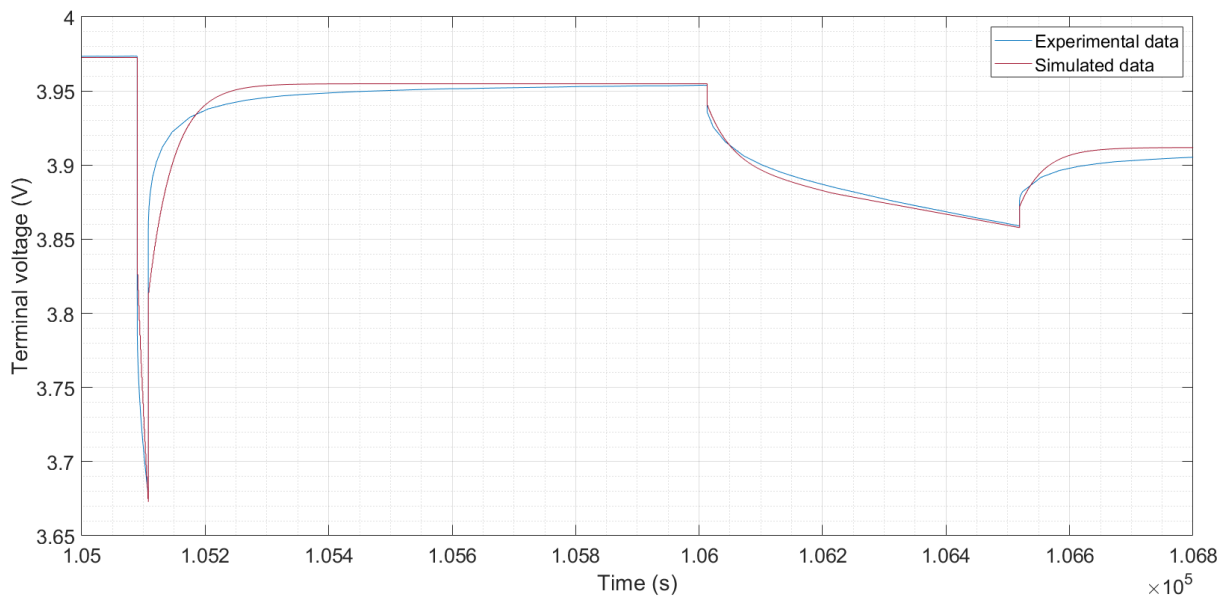

Figure 7.3: Result of tuning the parameters of 1RC model ($R_{int} = 0.7$ mΩ, $C_1 = 20$ kF and $R_1 = 2$ mΩ).

The obtained parameters that would be used for the results generation in next sections are the following ones:

- $R_{int} = 0.7$ mΩ
- $C_1 = 20$ kF
- $R_1 = 2$ mΩ

7.1.2. Simulation results for the pulse experiment

Simulation results of 1RC model are shown in Figure 7.3, where the orange solid line represents the simulation output voltage and the solid blue line represents the measured voltage value. We can see that the simulated data fit the experimental data with an acceptable accuracy. Notice that we can see slightly larger deviations when the battery is being charged periodically compared to the discharge portion. This could indicate to some additional phenomena presented in the charging portion.
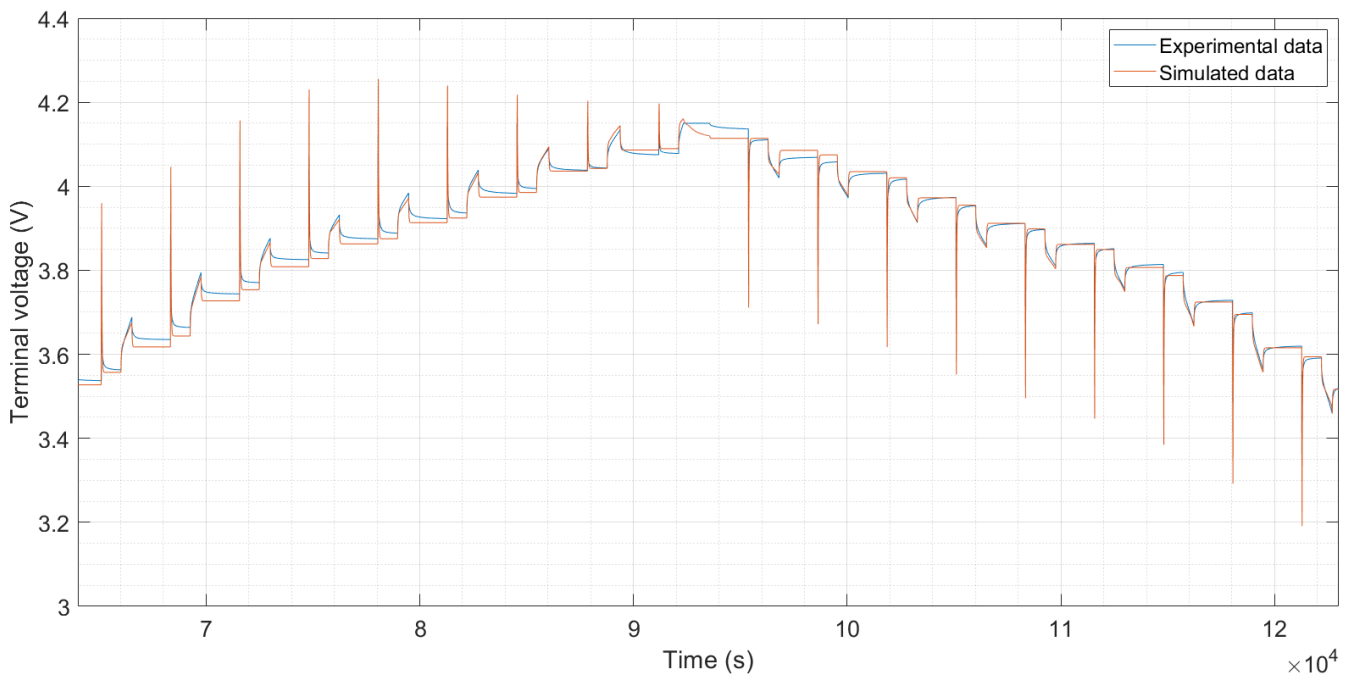

Figure 7.4: Simulated voltage of the battery obtained in 1RC model and experimental voltage of the battery under the pulse experiment.

In order to perform a quantitative analysis, and not qualitative, of the accuracy obtained in the results, the relative deviation of the voltage response between the simulated and experimental data has been calculated throughout the whole sample (Figure 7.5). The mean relative deviation for this case is 0.26 %.
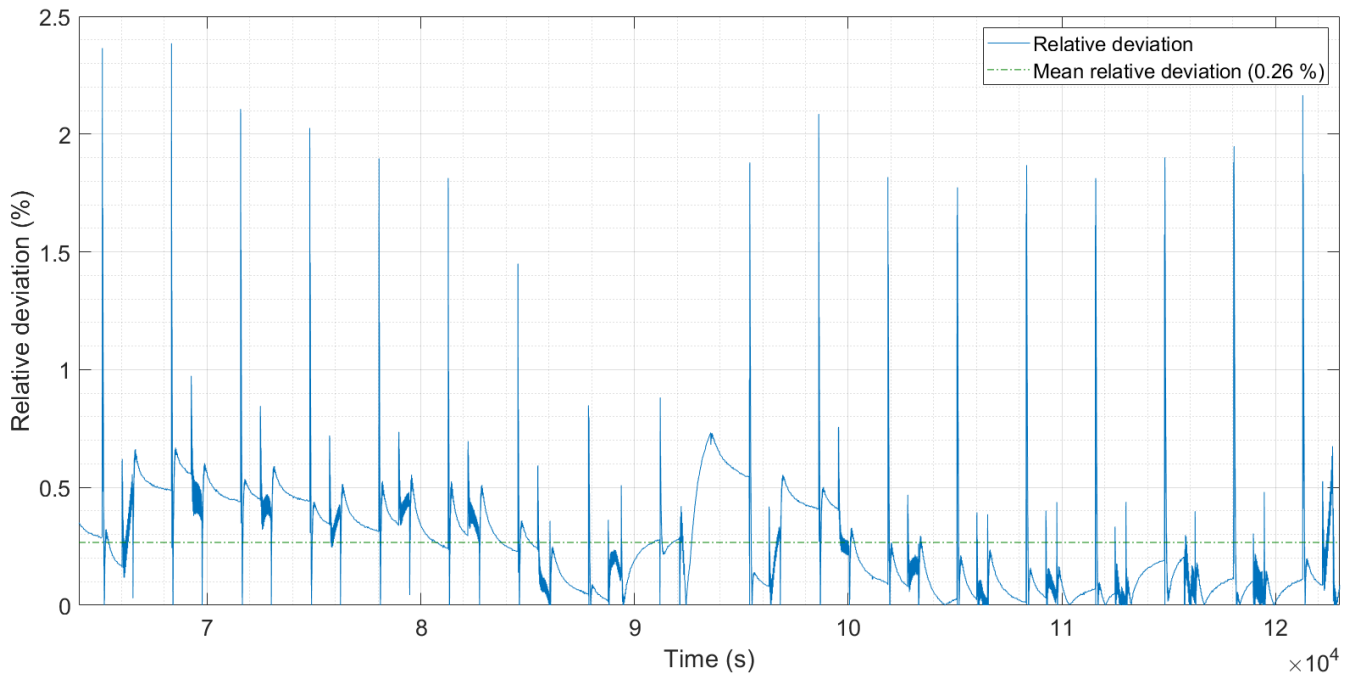
Figure 7.5: Relative deviation of the simulated voltage throughout time in 1RC model under the pulse experiment.

7.1.3. Simulation results for the dynamic experiment

Simulation results of 1RC model are shown in Figure 7.5, where the orange solid line represents the simulation output voltage and the solid blue line represents the measured voltage value. Notice that in the dynamic experiment, the response of the model looks like less accurate than in the pulse experiment. This may be due to the fact that most of the dynamic current pulses of the experiment are very sudden and represent large C rates up to 5C rate (Figure 7.1). As we saw in Section 7.1.1, the model was not very accurate when modelling the response of the battery under large and fast current level changes.

In order to do a quantitative analysis of the accuracy in the obtained results, the relative deviation of the voltage response between the simulated and the experimental data has been calculated throughout time (Figure 7.7). The mean relative deviation is 0.4 %, which supports the qualitative analysis of the accuracy done in the previous paragraph.
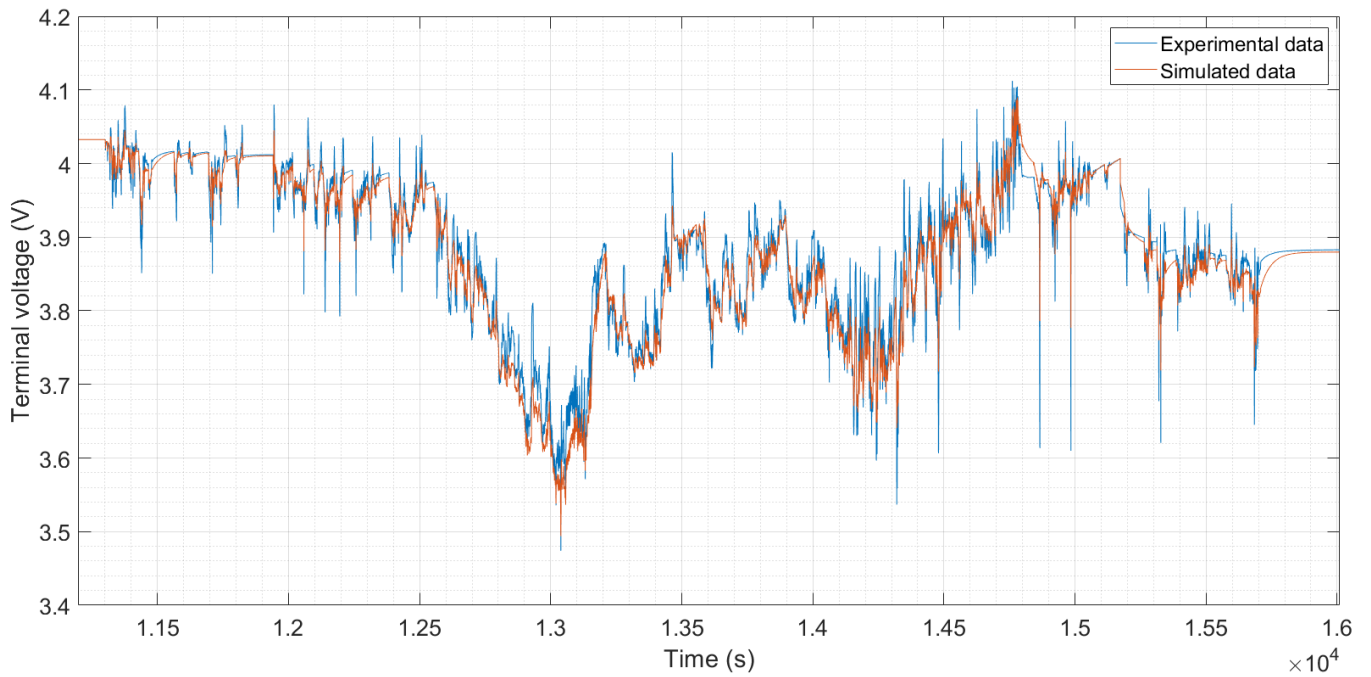
Figure 7.6: Simulated voltage of the battery obtained in 1RC model and experimental voltage of the battery under the dynamic experiment.
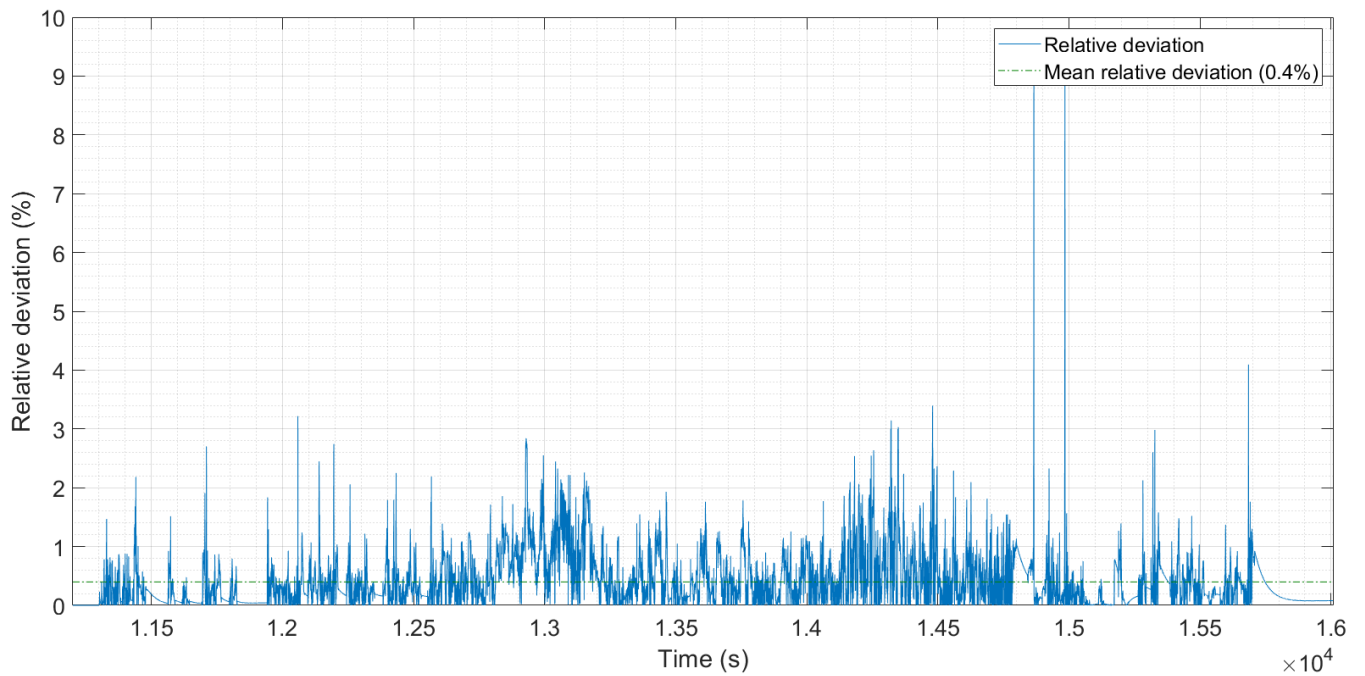

Figure 7.7: Relative deviation of the simulated voltage throughout time in 1RC model under the dynamic experiment.

7.2. Simulation results for 2RC

Regarding 2RC model, if the parameters are properly tuned, it is expected that we have better results than 1RC model. This is because an extra RC parallel circuit may provide better dynamic response than 1RC model by featuring additional frequency response.

7.2.1. Tuning of parameters

The result of tuning the parameters for 2RC model is shown in Figure 7.8. Note that the selection of parameters has been successfully since the simulated response voltage of the battery follows the measured response voltage of the battery very well. There has been an improvement of the model in the phase of relaxation voltage if we compare 2RC model to 1RC model. Regarding the voltage drop phase, the model shows a high accuracy following the measured data.
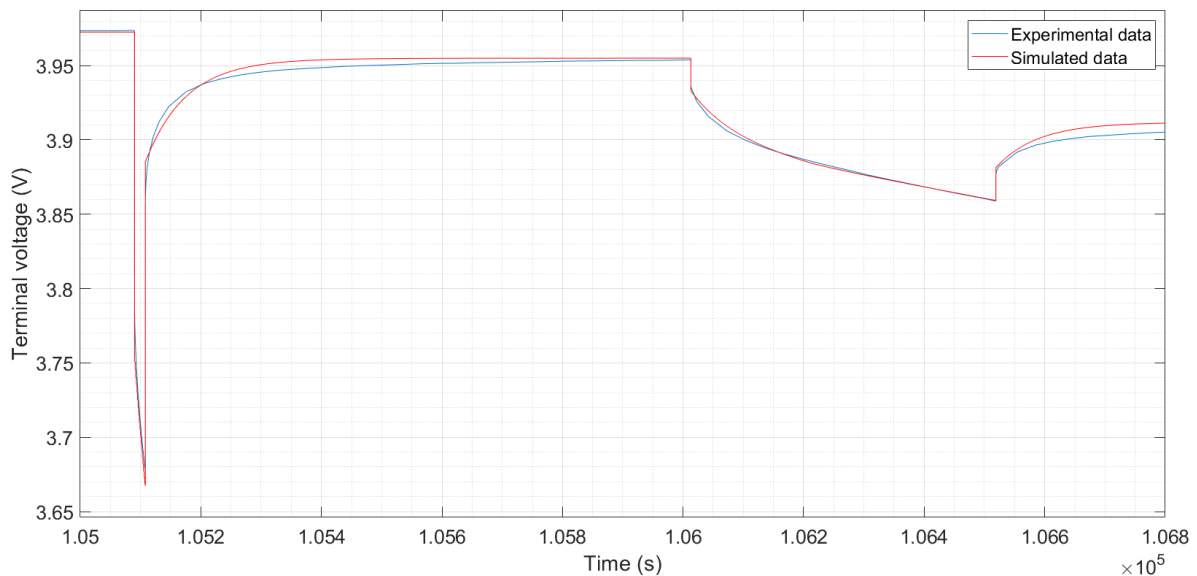

Figure 7.8: Result of tuning the parameters for 2RC model (R_{int} = 1.1 mΩ, C_1 = 53 kF, R_1 = 1.2 mΩ, C_2 = 284 kF and R_2 = 0.3349 mΩ).

Despite the high accuracy of the model, notice that this accuracy might be improved in the phase of forced regime as well as in the phase of relaxation voltage where the model reaches the steady state faster than experimental data.

The obtained parameters that would be used for the results generation in next sections are the following ones:
- R_{int} = 1.1 mΩ
- C_1 = 53 kF
- R_1 = 1.2 mΩ
- C_2 = 284 kF

- $R_2 = 0.3349$ mΩ

7.2.2. Simulation results for the pulse experiment

Simulation results of 2RC model are shown in Figure 7.9, where the orange solid line represents the simulation output voltage and the solid blue line represents the measured voltage value.
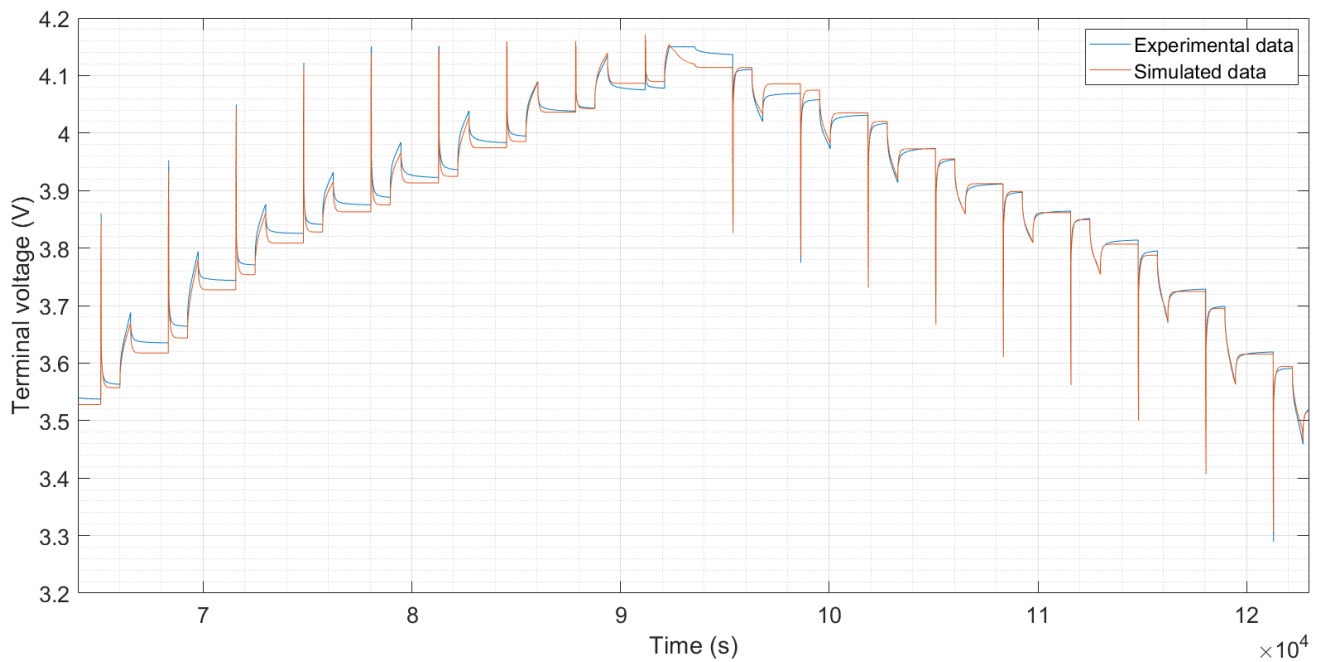

Figure 7.9: Simulated voltage of the battery obtained in 2RC model and experimental voltage of the battery under the pulse experiment.

Notice that the model is more accurate when the battery is being discharged than when the battery is being charged maybe due to the fact that some additional phenomena presented in the charging portion as it was already commented in Section 7.1.2.

In order to clarify if 2RC model is generally more accurate than 1RC model, the deviation between the simulated and experimental data has been calculated throughout the whole sample of time (Figure 7.10). The mean relative deviation is 0.25% what means that the accuracy has been improved (mainly in the forced regime) and hence, 2RC model is more accurate than 1RC model under periodical current pulses.
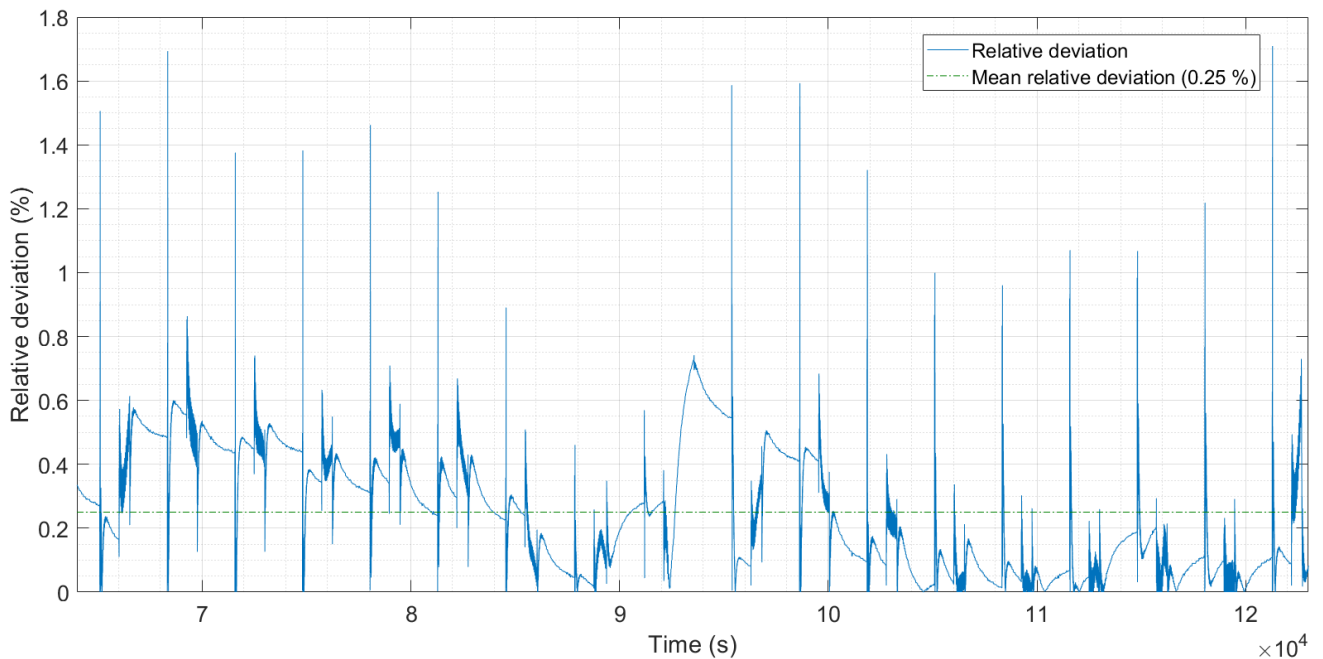
Figure 7.10: Relative deviation of the simulated voltage throughout time in 2RC model under the pulse experiment.

7.2.3. Simulation results for the dynamic experiment

Simulation results of 2RC model are shown in Figure 7.11, where the orange solid line represents the simulation output voltage and the solid blue line represents the measured voltage value. It is expected that Figure 7.8 shows a better fitting of the dynamic response of the battery than Figure 7.3.

In order to verify that 2RC model fits the behaviour of the battery under dynamic pulse currents better than 1RC model, a calculation of the deviation between measured and simulated data has been carried out (Figure 7.12). The mean relative deviation is 0.28% which confirms the statement that in general, when two RC circuits are included in the model, higher is the obtained accuracy when simulating.

Notice that there are some peaks of relative deviations (around 9% and 4%) that are caused by sudden high current discharging peaks that are hard to follow by the model.
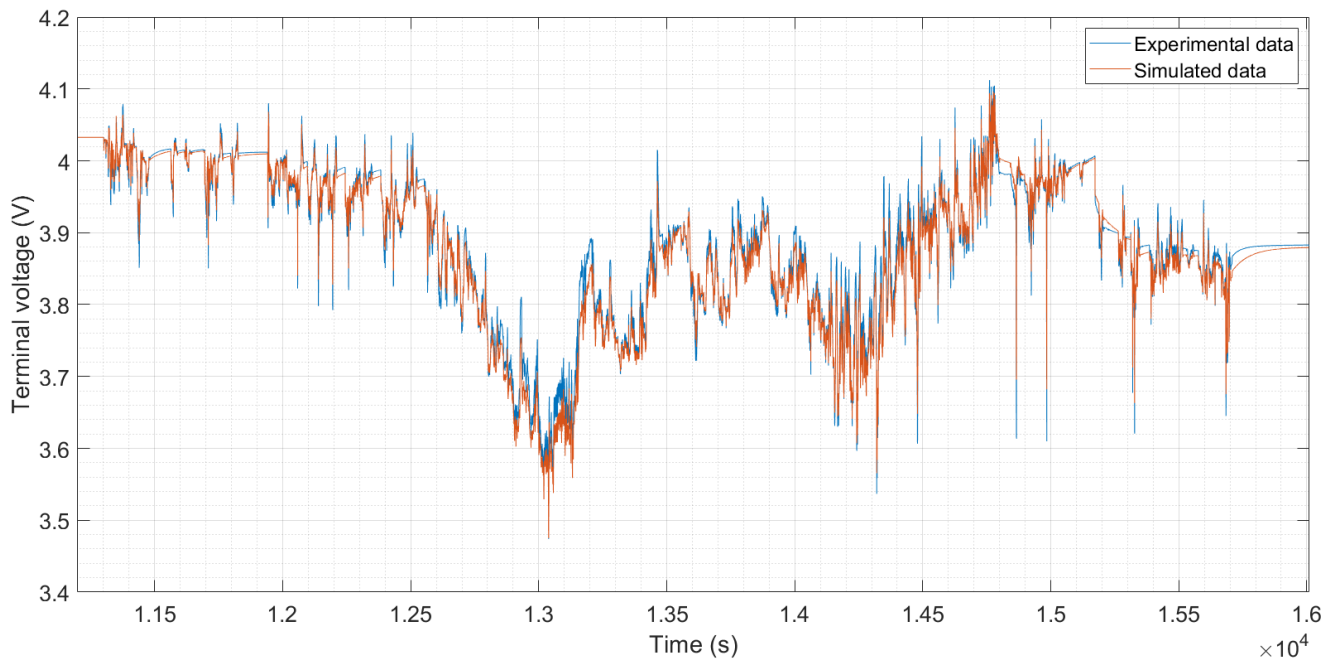
Figure 7.11: Simulated voltage of the battery obtained in 2RC model and experimental voltage of the battery under the dynamic experiment.
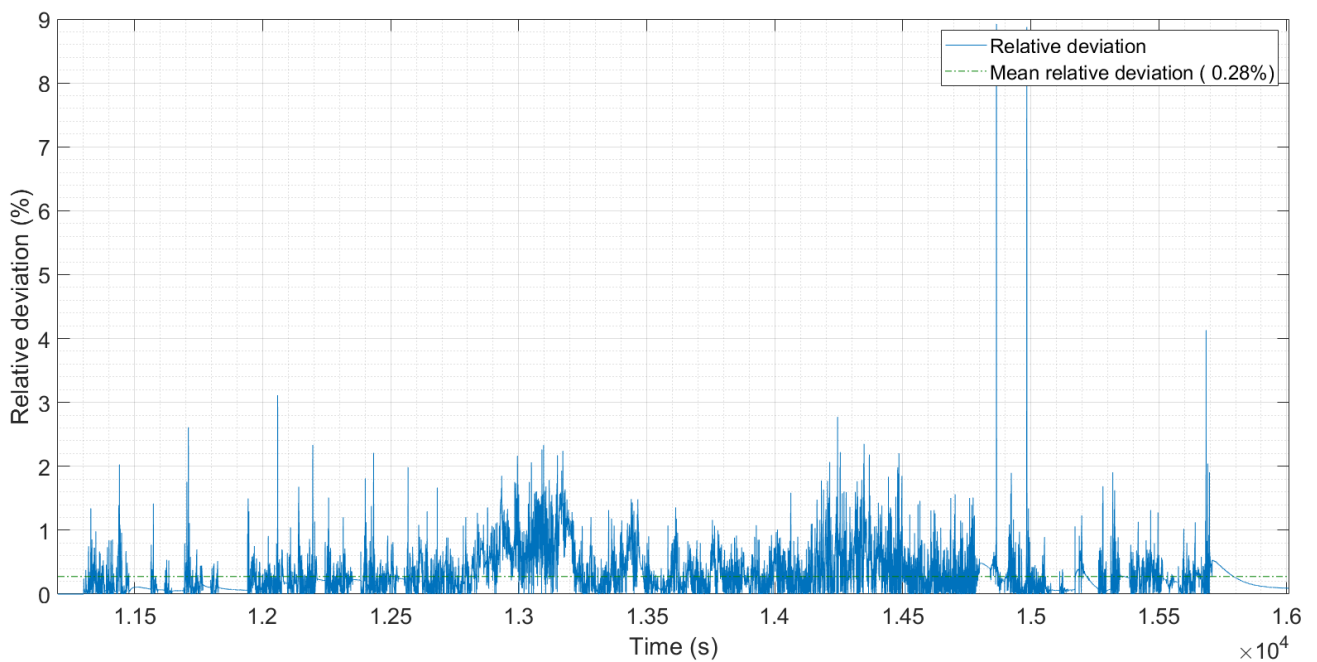

Figure 7.12: Relative deviation of the simulated voltage throughout time in 2RC model under the dynamic experiment.

7.3. Simulation results for 3RC model

As it has been commented in previous subsections, if the parameters are well tuned, this model should be the one with the highest accuracy. Anyway, it is increasingly difficult to handle six variable inputs by hand. Consequently, for further work and development an automatic fitting procedure should be necessary.

7.3.1. Tuning of parameters

The result of tuning the parameters for 3RC model is shown in Figure 7.13. Note that the selection of parameters was successful since the simulated response voltage of the battery follows the measured response voltage of the battery very well.
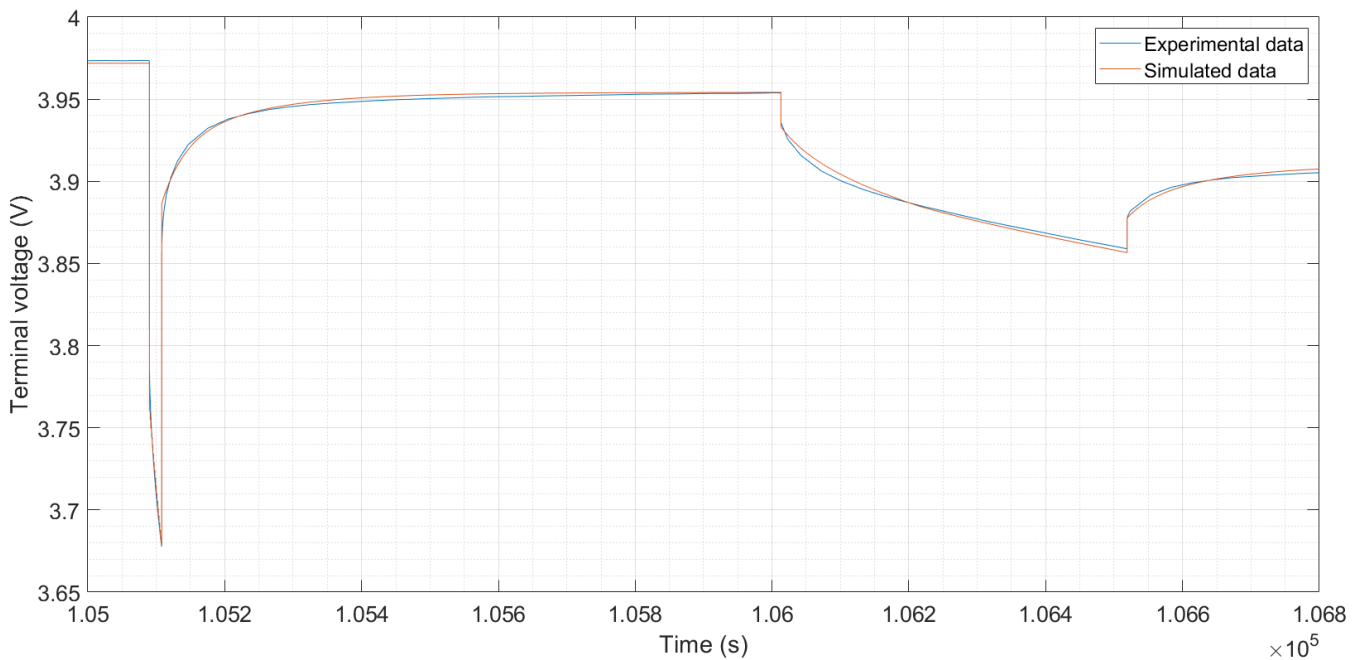
Figure 7.13: Result of tuning the parameters for 3RC model (R_{int} = 1.05 mΩ, C_1 = 100 kF, R_1 = 1.2 mΩ, C_2 = 3940 kF, R_2 = 0.33 mΩ, C_3 = 80 kF and R_3 = 0.4 mΩ).

The obtained parameters that would be used for the results generation in next sections are the following ones:
- R_{int} =1.05 mΩ
- C_1 = 100 kF
- R_1 = 1.2 mΩ
- C_2 = 3940 kF
- R_2 = 0.33 mΩ
- C_3 = 80 kF
- R_3 = 0.4 mΩ

7.3.2. Simulation results for the pulse experiment

Simulation results of 3RC model are shown in Figure 7.14, where the orange solid line represents the simulation output voltage and the solid blue line represents the measured voltage value.
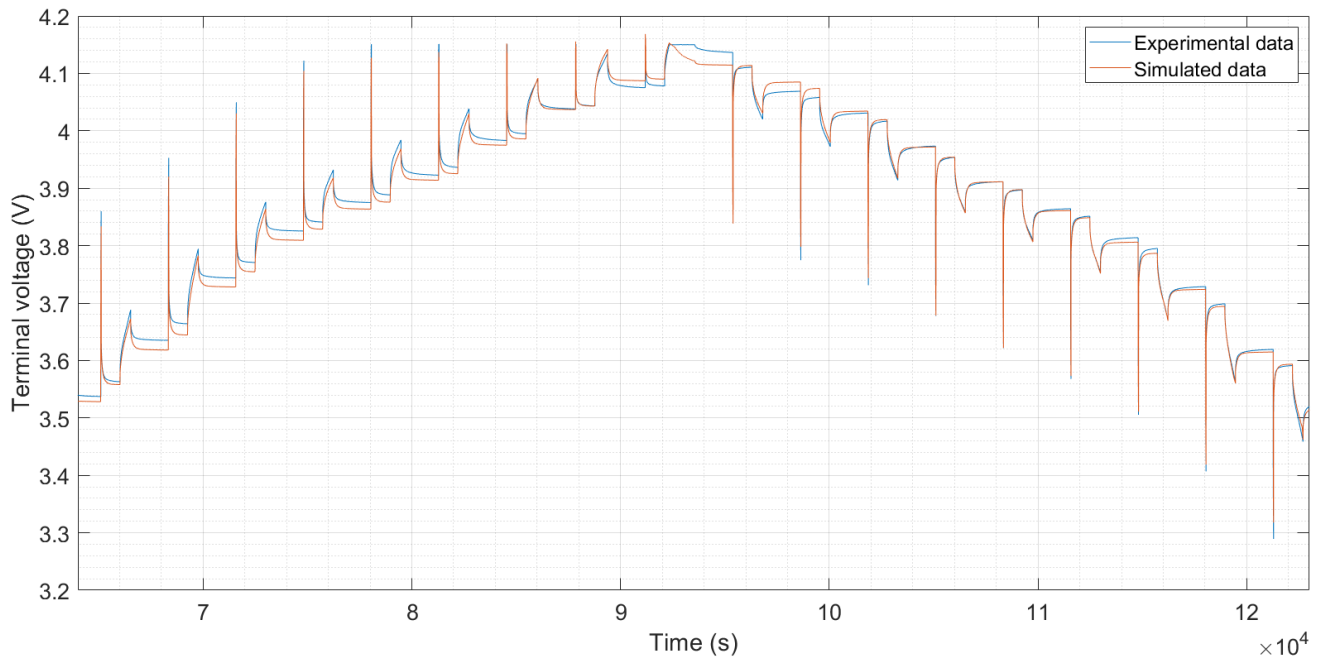

Figure 7.14: Simulated voltage of the battery obtained in 3RC model and experimental voltage of the battery under the pulse experiment.

Theoretically, if the parameters have been well tuned, 3RC model should be more accurate than 2RC model because in general higher order of RC model would feature higher accuracy [4]. In order to clarify if 3RC model is more accurate than 2RC model, the deviation between the simulated and experimental data has been calculated throughout the whole sample of time (Figure 7.15). The mean relative deviation is 0.23% what means that the accuracy has been improved and hence, 3RC model is more accurate than 2RC model under periodical current pulses. This higher accuracy is mainly due to the improvement of the relaxation voltage phase response of the model in comparison to 2RC and 1RC models.

There are some relative deviation spikes (up to 1.8 %) that are a consequence of rapid and high current changes that are hard to follow by the model. In the same way as was commented in previous sections,
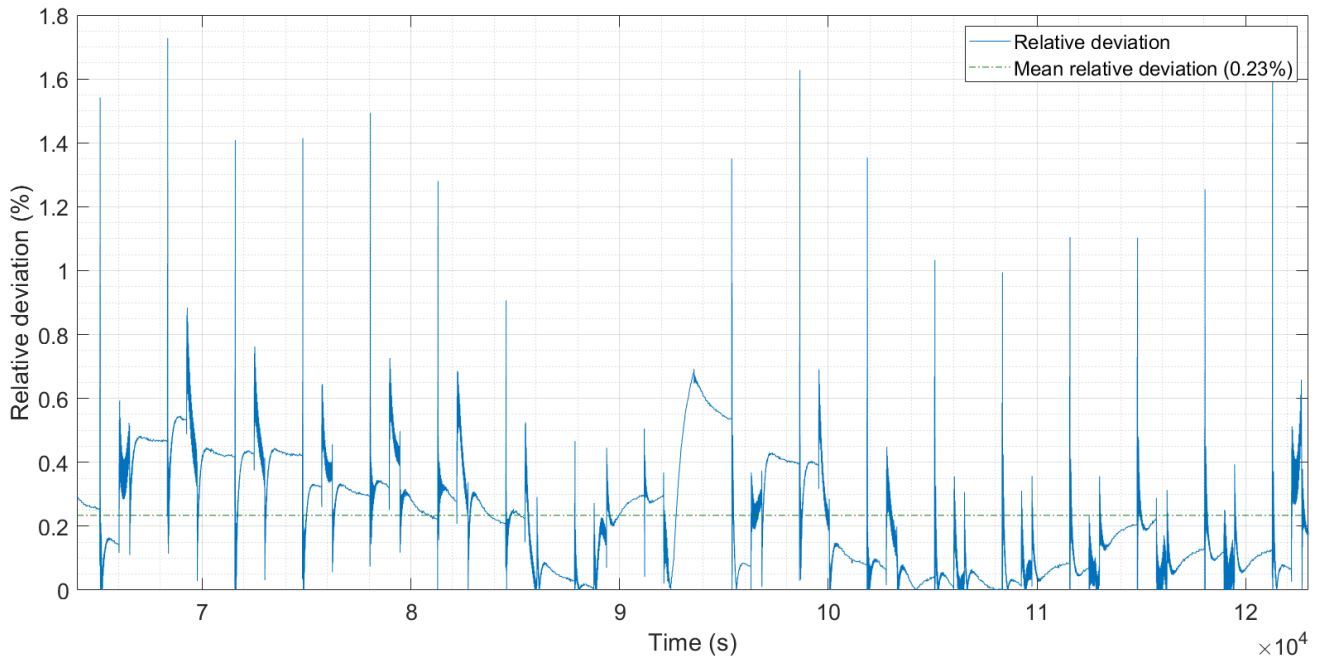
Figure 7.15: Relative deviation of the simulated voltage throughout time in 3RC model under the pulse experiment.

7.3.3. Simulation results for the dynamic experiment

Simulation results of 3RC model are shown in Figure 7.16. The accuracy of the model seems to be high, but it cannot be said whether 3RC model is more accurate than 2RC model under dynamic current pulses. That is why a calculation of the deviation throughout the whole sample of time has been carried out (Figure 7.17). The mean relative deviation is 0.23%. This means that 3RC model is more accurate than 2RC model under dynamic current pulses because the electrochemical phenomena that take place inside the battery (Section 2.3) are represented in a greater detail.

Figure 7.16: Simulated voltage of the battery obtained in 3RC model and experimental voltage of the battery under the dynamic experiment.

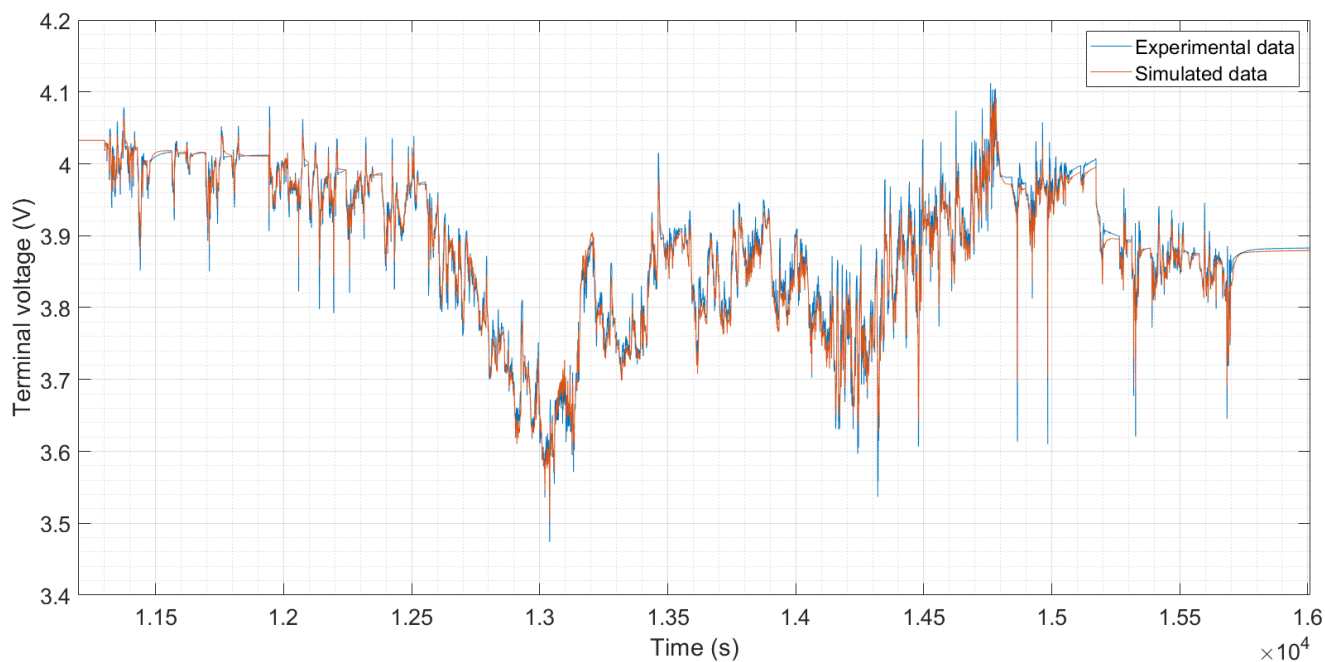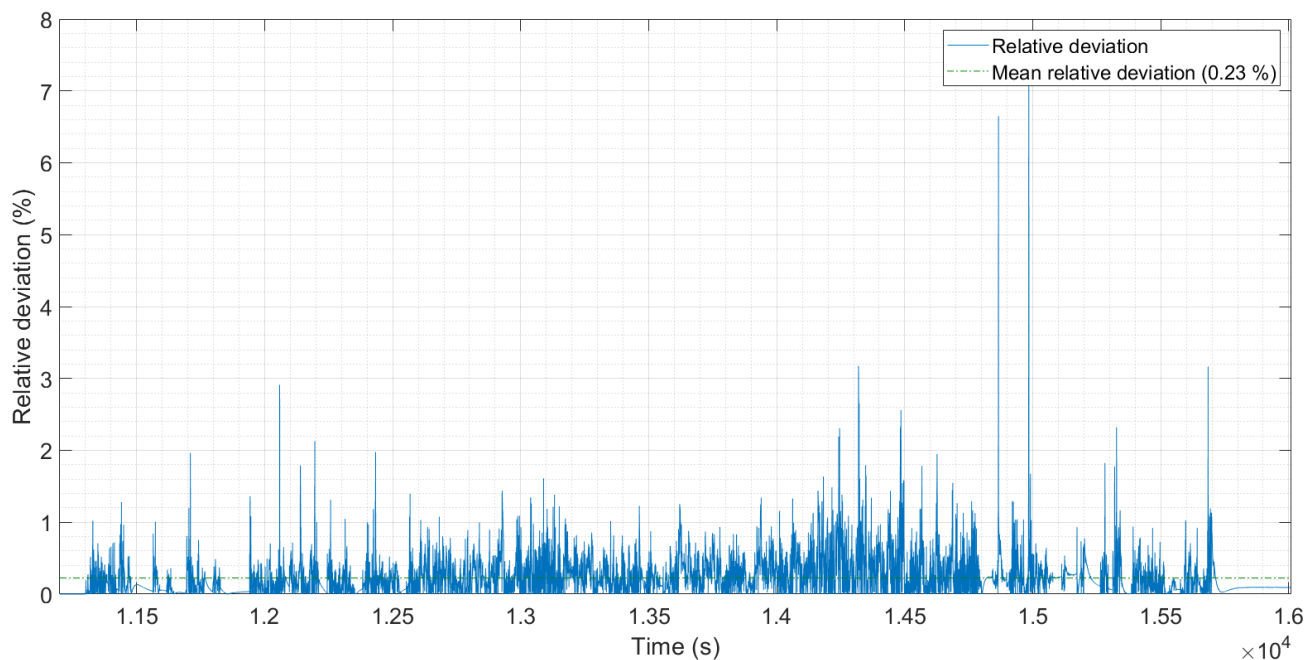Figure 7.17: Relative deviation of the simulated voltage throughout time in 3RC model under the dynamic experiment.

7.4. General comments about the results

In this section, we are going to put all results together and try to give a general overview of the results obtained.

First of all, results of the three models for the pulse experiment are going to be compared, selecting a reduced sample time (Figure 7.18). In this figure, it is shown the response of the terminal voltage of the battery following a discharge current pulse (0.5C rate). Notice that the model that fits better the experimental data in all phases (voltage drop, forced regime and relaxation voltage) is 3RC model.
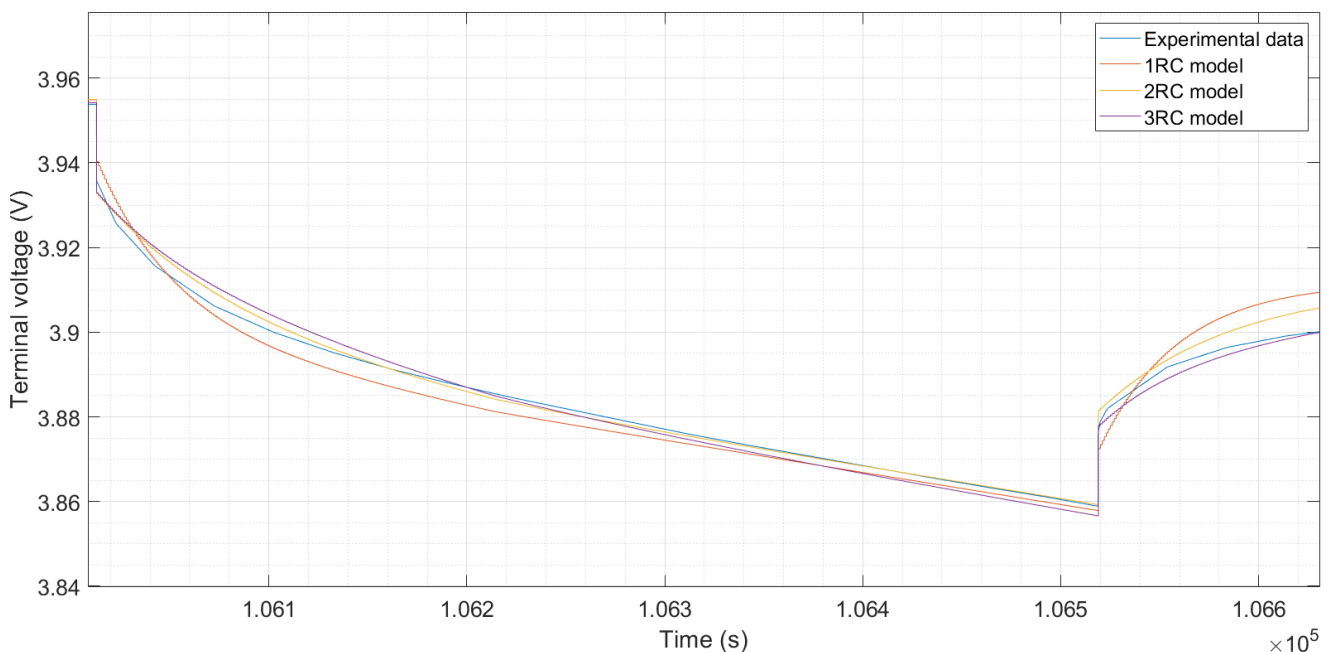

Figure 7.18: Comparison of the simulation outputs of the different models for the pulse experiment.

Regarding the dynamic experiment we can say that we have successfully chosen the parameters because the mean relative deviation has been reduced when modelling higher order RC models. In order to verify this statement, we have plotted the three models in the same graphic and we have zoomed into the graphic to see in detail the accuracy of every model (Figure 7.19).

What we can get from the figure is that 3RC model seems to be the most accurate as it is always the closest one to the real output voltage and the same happens with 2RC model. Then, we can conclude that the tune of parameters has been successful due to the fact that the higher is the order of the RC network, the higher has been the obtained accuracy. However, the tuning of parameters could have been even better if we would have used the provided EIS data to determine the parameters of the models. This way of determining the parameters for the model involved taking into account the dependency of the parameters on SoC, and this would have increased the complexity of this work.
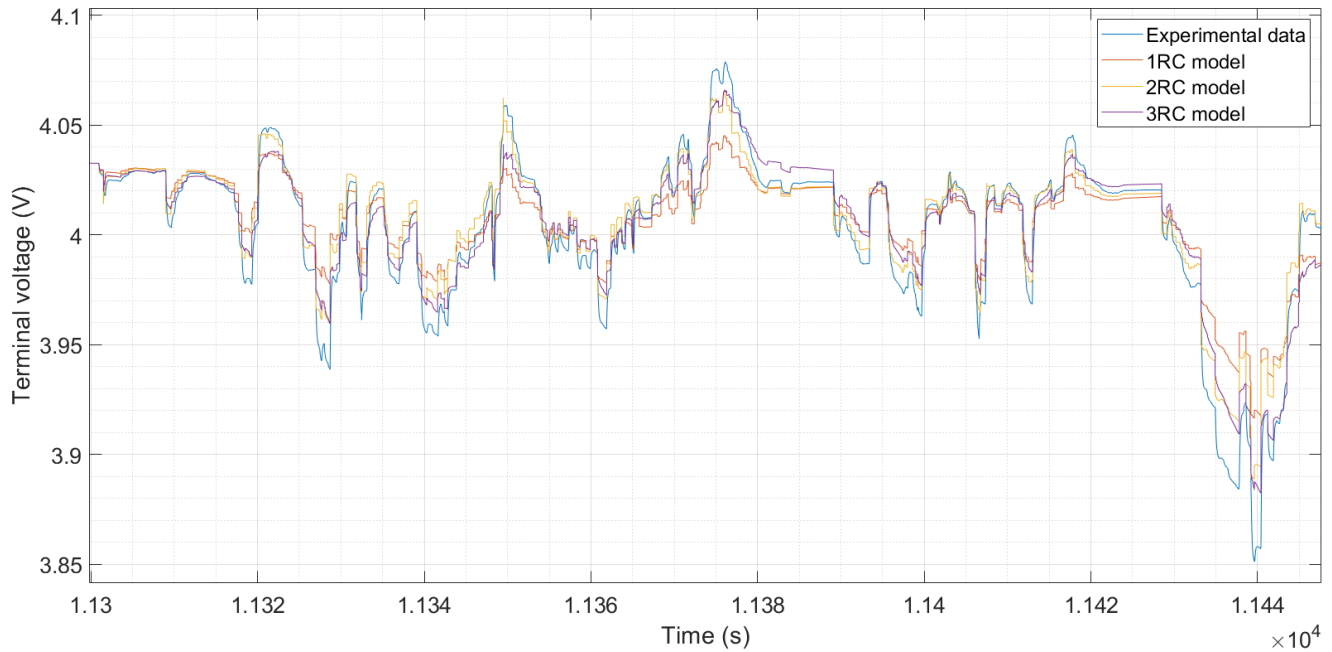
Figure 7.19: Comparison of the simulation outputs of the different models for the dynamic experiment.

In order to confirm quantitatively that in this work higher RC models suppose a higher accuracy when modelling, Table 7.1 includes selection of the obtained results. In this table, Deviation 1 refers to mean relative deviation in the pulse experiment and Deviation 2 refers to mean relative deviation in the dynamic experiment.

Table 7.1: Collection of obtained results.

Model	R_{int} (mΩ)	C_1 (kF)	R_1 (mΩ)	C_2 (kF)	R_2 (mΩ)	C_3 (kF)	R_3 (mΩ)	Deviation 1 (%)	Deviation 2 (%)
1RC	0.7	20	2	-	-	-	-	0.26	0.4
2RC	1.1	53	1.2	284	0.3349	-	-	0.25	0.28
3RC	1.05	100	1.2	3940	0.33	80	0.4	0.23	0.23

7.5. Sensitivity analysis

In this section, we have analysed how the parameters of the models affect its accuracy by performing a sensitivity analysis.

7.5.1. Sensitivity analysis for pulse experiment

For performing the sensitivity analysis of the battery models (1RC and 2RC models) following a discharge current pulse, we are going to use the sample seen in Figure 6.1.

7.5.1.1. Sensitivity analysis for 1RC model

In this subsection, two cases will be studied to see how the variation of parameters affect the response of the terminal voltage of the battery. The performed analysis will be compared to Figure 7.3. The next cases will be studied in this subsection:

Case 1: In this case, the resistor defined as R_1 will be divided by 10. This also means that the time constant defined as $\tau_1 = R_1 C_1$ will be also divided by 10.

Case 2: In this case, the internal resistance of the battery represented by R_{int} will be divided by 2.
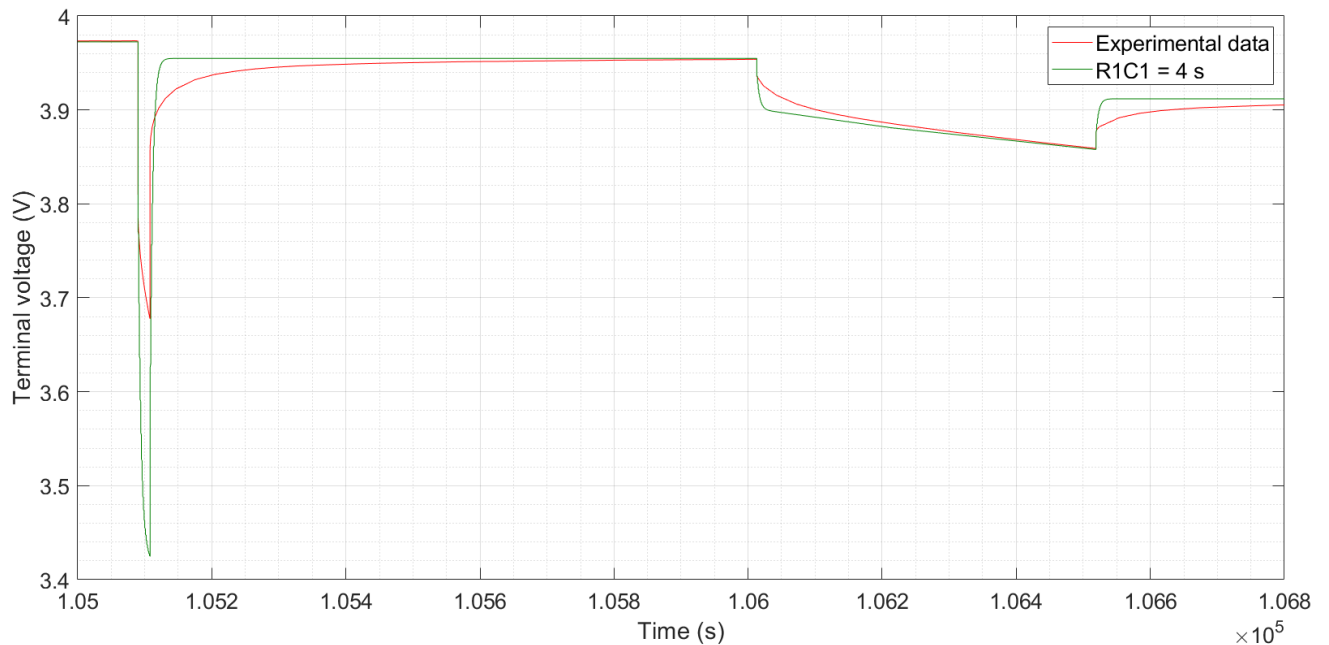
Figure 7.20: Output voltage of 1RC model in Case 1.

Since the time constant τ_1 has been reduced 10 times, the relaxation voltage and the forced regime are sharper and reach the steady state sooner than the experimental data. This is due to the fact that time constant, i.e. response of the RC circuit is faster than electrochemical phenomena inside the battery. For example, polarization and mass transfer, have very slow dynamics and occur during hours of relaxation phase [46]. Consequently, the voltage variation after a period of discharge of the real battery is longer and smoother than the one in the model.

Figure 7.21: Output voltage of 1RC model in Case 2.

By changing the internal resistance of the battery, we realise that this parameter is directly related to the voltage drop phase and can be observed when the load current level changes.

7.5.1.2.   Sensitivity analysis for 2RC model

In this subsection, three cases will be studied to see how the parameters affect the response of the terminal voltage of the battery. The performed analysis will be compared to Figure 7.8. The next cases will be studied in this subsection:

Case 1: In this case, the resistor defined as R_1 will be divided by 10. This also means that the time constant defined as $\tau_1=R_1C_1$ will be also divided by 10.

Case 2: In this case, the resistor defined as R_2 will be divided by 10. This also means that the time constant defined as $\tau_2=R_2C_2$ will be also divided by 10.

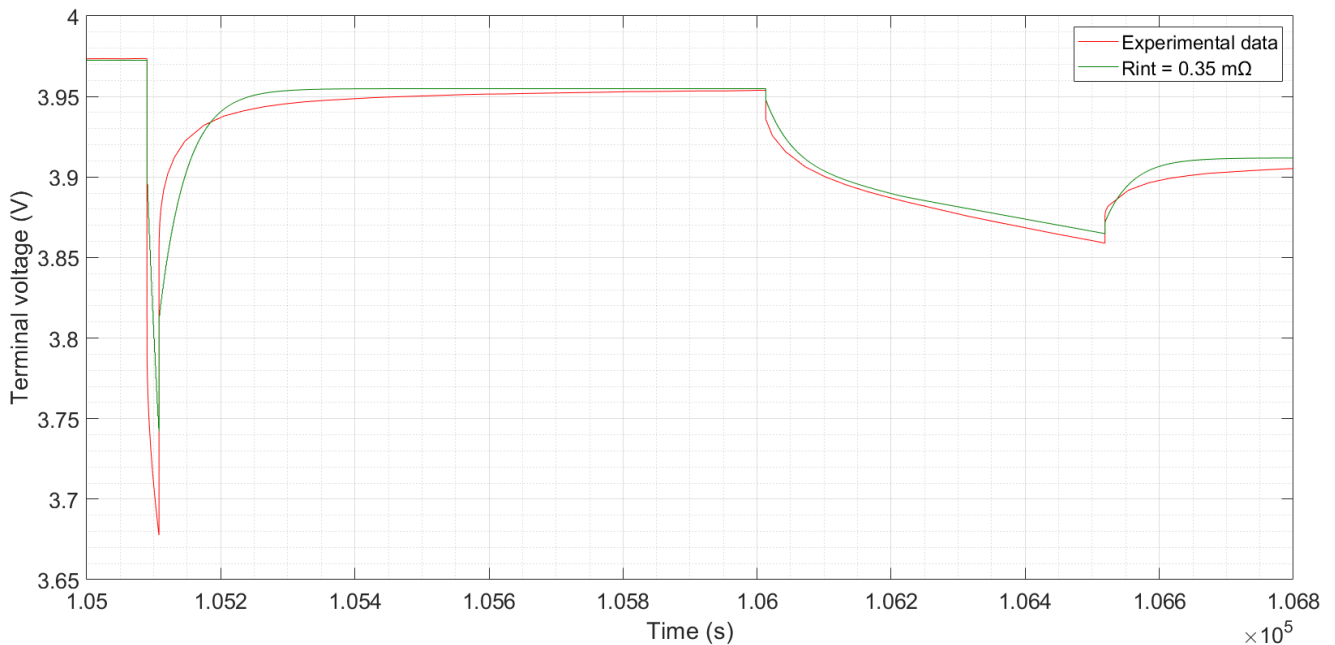**Case 3:** In this case, the internal resistance of the battery represented by R_{int} will be divided by 2.

In Figure 7.22, we can see the same that was commented in Section 7.5.1.1. The dynamic response of the battery is not adequate since time of relaxation voltage in the real battery is longer.

In Figure 7.23, we can see that the accuracy of the model barely changes, although it can be seen that the output of the model is faster than the measured data in the relaxation voltage phase. Besides, notice that the model presents a slightly deviation from the measured data in the forced regime phase.

In Figure 7.24, we can see almost the same that was commented previously in 7.5.1.1. A change in the internal resistance of the battery affects directly the voltage drop phase.
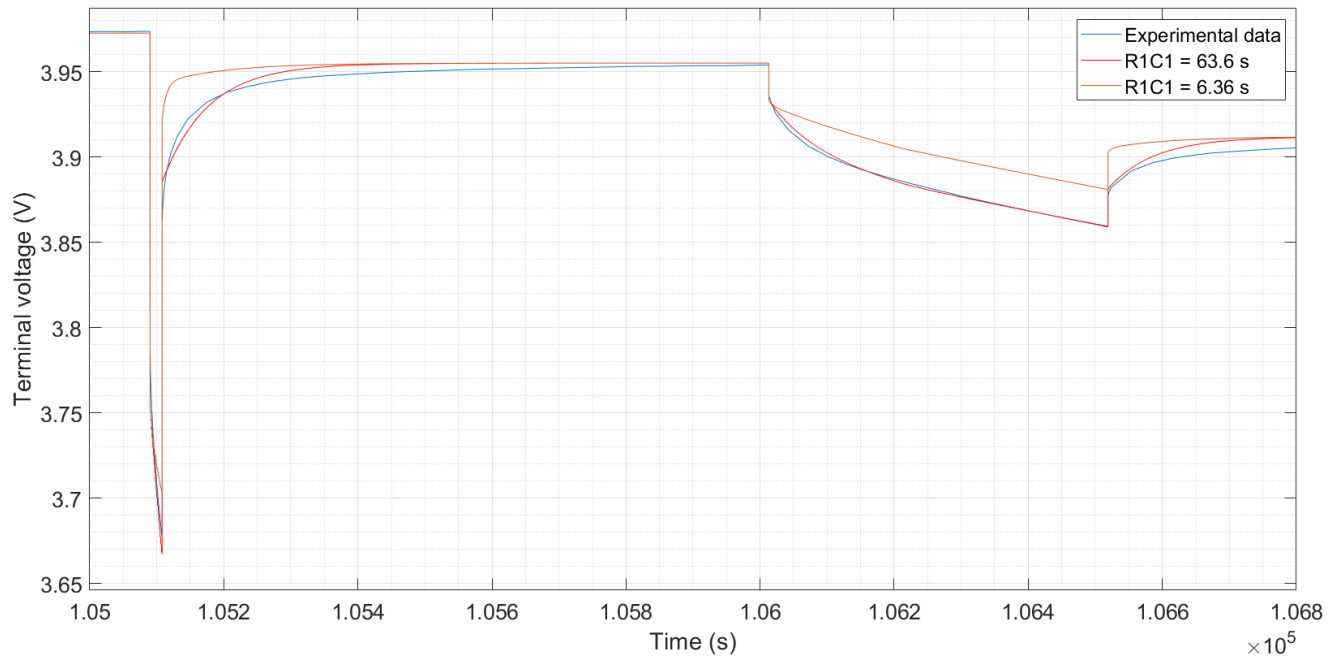
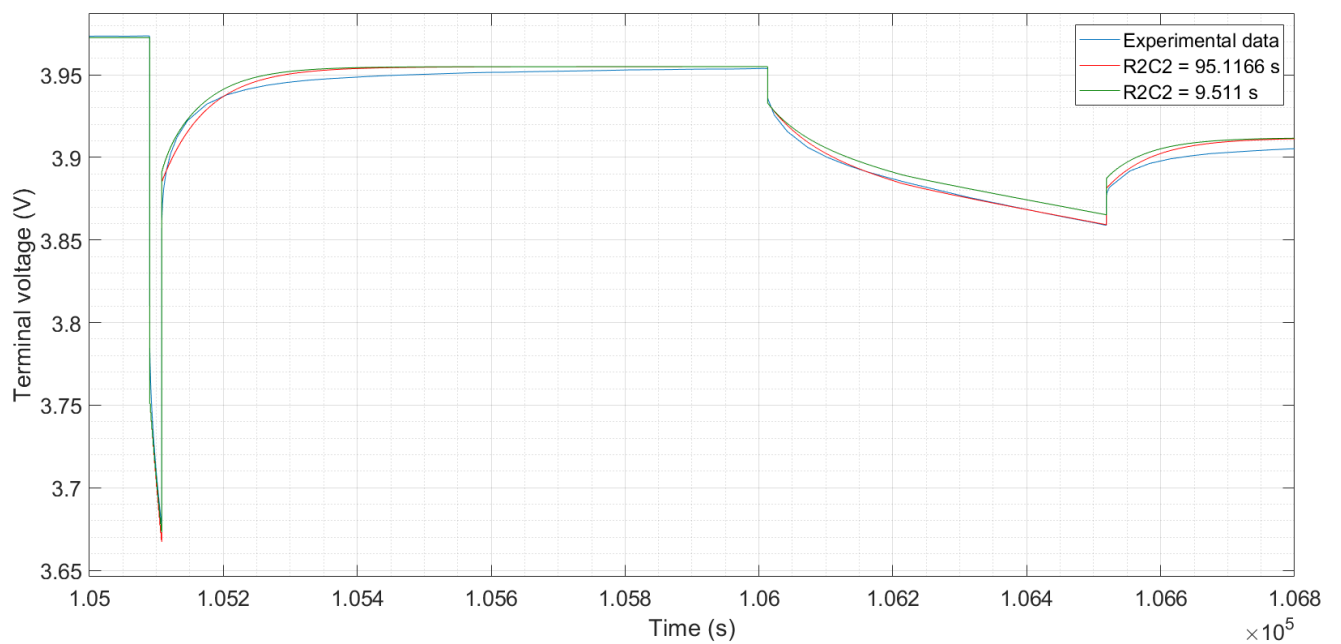Figure 7.22: Output voltage of 2RC model in Case 1.

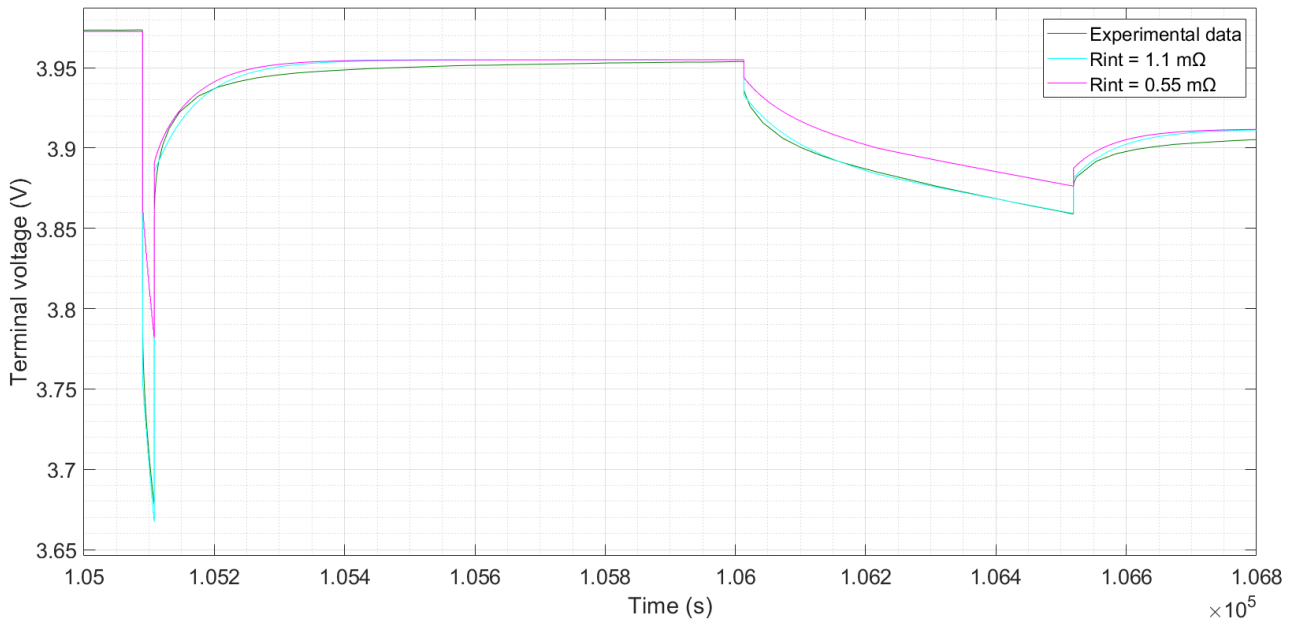Figure 7.23: Output voltage of 2RC model in Case 2.

Figure 7.24: Output voltage of 2RC model in Case 3.

7.5.2. Sensitivity analysis for dynamic experiment

In order to carry out this parameter sensitivity analysis, we are going to consider 2RC model shown in Figure 3.7. In this subsection, the following set of parameters $\{R_{int}, C_1, R_1, C_2, R_2\}$ is going to be analysed.

This parameter sensitivity analysis is going to be divided into 4 cases:

Case 1: This first case is going to be considered as the most accurate case.
$\{R_{int} = 0.7 \text{ m}\Omega, C_1 = 5.3 \text{ kF}, R_1 = 1.2 \text{ m}\Omega, C_2 = 204 \text{ kF}, R_2 = 0.2349 \text{ m}\Omega\}$

Case 2: In this second case we are going to keep all the parameters constant except R_2 that is going to be multiplied by 10.
$\{R_{int} = 0.7 \text{ m}\Omega, C_1 = 5.3 \text{ kF}, R_1 = 1.2 \text{ m}\Omega, C_2 = 204 \text{ kF}, R_2 = 2.349 \text{ m}\Omega\}$

Case 3: In this third case we are going to keep all the parameters constant except R_1 that is going to be multiplied by 10.
$\{R_{int} = 0.7 \text{ m}\Omega, C_1 = 5.3 \text{ kF}, R_1 = 12 \text{ m}\Omega, C_2 = 204 \text{ kF}, R_2 = 0.2349 \text{ m}\Omega\}$

Case 4: In this fourth case we are going to keep all the parameters constant except R_{int} that is going to be multiplied by 10.
$\{R_{int} = 7 \text{ m}\Omega, C_1 = 5.3 \text{ kF}, R_1 = 1.2 \text{ m}\Omega, C_2 = 204 \text{ kF}, R_2 = 0.2349 \text{ m}\Omega\}$

The results of the different cases in a selected sample are shown in Figure 7.25. It can be seen that the model output is most sensitive to the variation of the internal resistance of the

battery (**Case 4**) as it would be expected, since the output is directly related to R_{int} as we can observe in the system of equations (3.3).The change of the internal resistance of the battery affects mainly the voltage drop. The change of R_1 (**Case 3**) is the second most important parameter in terms of sensitivity. Then, we can observe that by changing R_2 (**Case 2**) we can observe a slight sensitivity in the dynamic response of the model following dynamic current pulses, but the model output is very close to the model in which parameters were tuned (**Case 1**).

In order to compare the results, we have calculated the relative deviation (%) in every case in Figure 7.26. As we can see the relative deviations give us the same information about the sensitivity. Sensitivity analysis proves that the output of 2RC model is most sensitive to R_{int} and R_1.
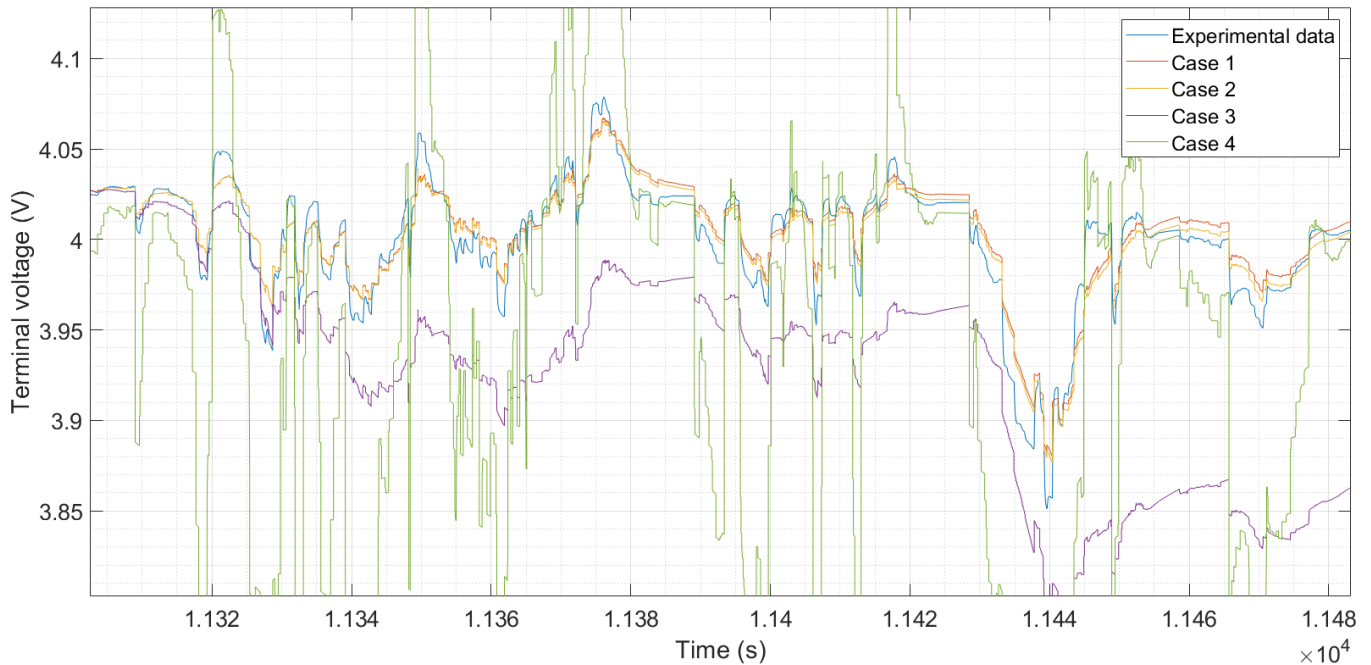

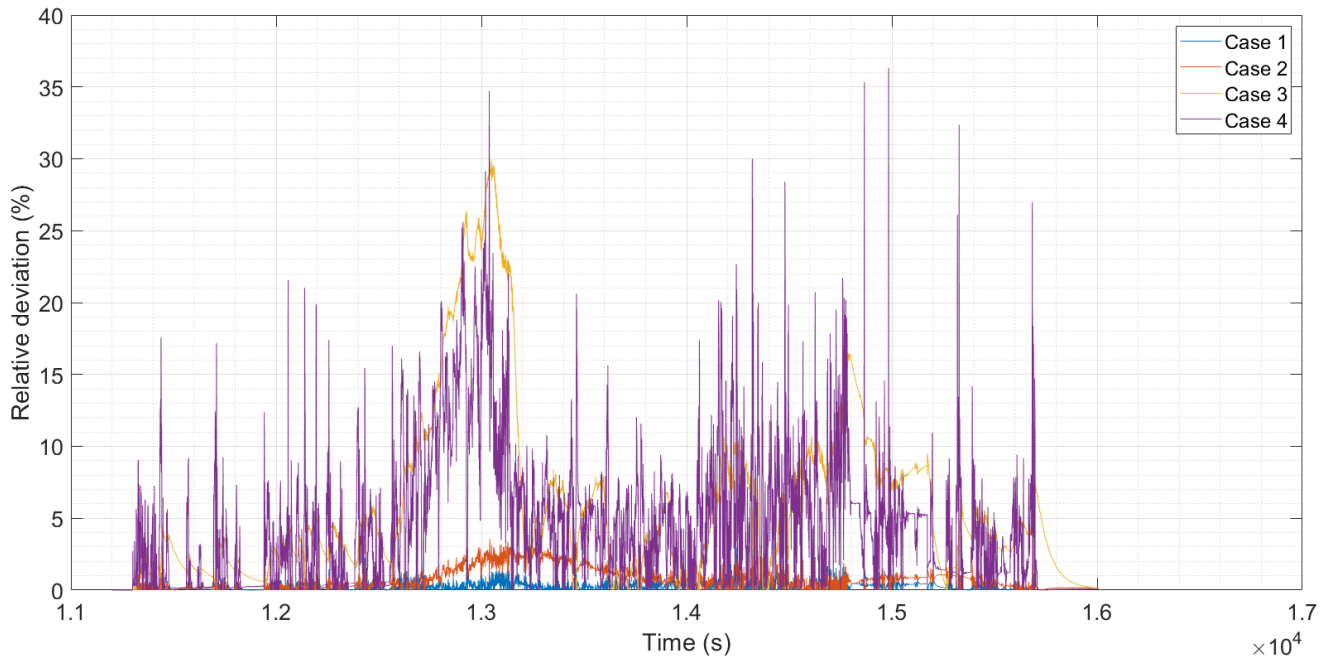Figure 7.25: Output voltage of the different cases.

Figure 7.26: Relative deviations of the different cases.

Now, we are going to explain the reason of different sensitivities found in this subsection from the electrochemical point of view. Benchmark case for this analysis will be **Case 1**, since it is the most accurate model and the parameters have been properly selected.

In **Case 3**, there is a substantial difference with **Case 1** due to the fact that we have increased R_1 by ten times and if we take a deep look in a typical Nyquist plot of a second order RC (Figure 4.2), the plot will be very different. The first semicircle will be bigger and as a consequence of this, the diffusion phenomena which are presented in the Nyquist plot as a straight line will be covered by this semicircle. By increasing R_1 there are no high frequency responses in the battery model which results in voltage drift.

In **Case 2**, there is not a major difference with **Case 1**. We have increased R_2 by ten times, however this parameter affects just the diffusion area (low frequencies).

In **Case 4**, there is a significant difference with **Case 1** since the Nyquist plot have been shifted to the right excessively and we can claim that this model does not represent the electrochemical phenomena that take place inside the battery.

8. Conclusions

1) We parameterised the three different ECMs in question.

2) We simulated the three different ECMs under two different representative operating conditions.

3) The obtained results indicate that the higher order is the model, the higher is the accuracy of the model if the parameters have been properly selected.

4) Nyquist plot of the models were compared to Nyquist plot provided in the EIS experiment.

5) Sensitivity analysis of different models under different scenarios was performed and we reached the conclusion that some parameters affect more the response of the model than others.

6) We related the sensitivity analysis of the models to electrochemistry reaching the conclusion that ECM parameters are a valid representation of electrochemical phenomena that take place inside the battery.

The maximum mean relative deviations of the three RC models under two representative operating conditions were all less than 0.4 %, which can generally satisfy the precision requirements for the practical engineering calculation, such as algorithms based on ECM for advanced BMSs.

Recommendations for future research

Our next work could be modelling the same ECMs taking into account the dependency of the parameters on the SoC and the temperature by carrying out different experiments where the Li-ion pouch cell was tested under different temperatures and SoCs. By adding this dependency, we could develop more accurate models to implement them to battery control units.

9. Bibliography

[1] Woosuk Sung and Chee BurmShin, "Electrochemical model of a lithium-ion battery implemented into an automotive battery management system," pp. 87-97.

[2] Xiaosong Hu,Huei Peng and Shengbo Li, "A comparative study of equivalent circuit models for Li-ion batteries," 2012, pp. 359-367.

[3] William Scott,Mehrdad Mastali,Leonardo Gimenez,Michael Fowler and Roydon Frasera, "Empirical Modeling of Lithium-ion Batteries Based on Electrochemical Impedance Spectroscopy Tests," 2015, pp. 169-177.

[4] Lijun Zhang, Hui Peng, Zhansheng Ning, Zhongqiang Mu and Changyan Sun , "Comparative Research on RC Equivalent Circuit Models for Lithium-Ion Batteries of Electric Vehicles," *applied sciences,* 28 September 2017.

[5] Uwe Westerhoff,Kerstin Kurbach,Frank Lienesch and Michael Kurrat, "Analysis of Lithium-Ion Battery Models Based on Electrochemical ImpedanceSpectroscopy," in *Energy Technology*, 2016, pp. 1620-1630.

[6] "Kyria," [Online]. Available: http://www.kyria.co.uk/blog-the-25th-anniversary-of-the-lithium-ion-battery/.

[7] "Battery University," 31 July 2017. [Online]. Available: http://batteryuniversity.com/learn/article/lithium_based_batteries.

[8] Zempachi Ogumi, Robert Kostecki, Dominique Guyomard, and Minoru Inaba, "Lithium-Ion Batteries-The 25th Anniversary of Commercialization".

[9] "infralogistica.es," 2017. [Online]. Available: http://intralogistica.es/?p=86.

[10] Jiuchun Jiang and Caiping Zhang, "Performance Modeling of Lithium-ion Batteries," in *Fundamentals and Applications of Lithium-ion Batteries in Electric Drive Vehicles*, 2015, pp. 9-10.

[11] "The electric energy," [Online]. Available: http://theelectricenergy.com/lithium-and-lithium-ion-battery/.

[12] D.-M. Duong, "DFT calculations for cathode materials of rechargeable Li-ion batteries," February 2014.

[13] "Sigma-Aldrich," [Online]. Available: https://www.sigmaaldrich.com/materials-science/material-science-products.html?TablePage=106039040.

[14] G. V. Research, Lithium-Ion Battery Market Analysis By Product (Lithium Cobalt Oxide, Lithium Iron Phosphate, NCA, LMO, LTO, Lithium Nickel Manganese Cobalt (NMC)), By Application, And Segment Forecasts, 2018 - 2025, 2017.

[15] "Battery University," [Online]. Available: http://batteryuniversity.com/learn/article/types_of_battery_cells.

[16] "Tanpo," [Online]. Available: http://www.global-tanpo.com/?t=view&id=68.

[17] "Farnell element 14," [Online]. Available: http://es.farnell.com/multicomp/lir2450/pila-de-bot-n-litio-120mah-3-6v/dp/2009025.

[18] "Electronic design," [Online]. Available: http://www.electronicdesign.com/.

[19] "Targray," [Online]. Available: https://www.targray.com/li-ion-battery/lithium-ion-cells.

[20] Y. Wu, "Lithium-ion Batteries: Fundamentals and Applications. ASME-SCVS Professional Development Series," vol. 23, 2015.

[21] EUROBAT, "Battery Systems for Electric Energy Storage Issues. Association of European Automotive and Industrial Battery Manufacturers," 2005.

[22] B. Mok, "Types of Batteries Used for Electric Vehicles," October 2017. [Online]. Available: http://large.stanford.edu/courses/2016/ph240/mok2/.

[23] A. Jossen, "Fundamental of battery dynamics," *Journal of power sources,* 2005.

[24] "All about circuits," [Online]. Available: https://www.allaboutcircuits.com/textbook/alternating-current/chpt-3/more-on-the-skin-effect/.

[25] M. Aslani, 14 December 2014. [Online]. Available: http://large.stanford.edu/courses/2012/ph240/aslani1/.

[26] "Office of Energy Efficiency & Renewable Energy," 14 September 2017. [Online]. Available: https://www.energy.gov/eere/articles/how-does-lithium-ion-battery-work.

[27] Seong Jin,Ana Jianlin Li,Claus Daniel Debasish Mohanty Shrikant Nagpure and David L.Wood, "The state of understanding of the lithium-ion-battery graphite solid electrolyte interphase (SEI) and its relationship to formation cycling," 2016.

[28] "Electronic Products," 2016. [Online]. Available: https://www.electronicproducts.com/Power_Products/Batteries_and_Fuel_Cells/What_are_dendrites_and_why_do_they_cause_fires_in_lithium_batteries.aspx.

[29] W.-Y. Chang, *The State of Charge Estimating Methods for Battery: A Review,* 2013.

[30] Kong Soon Ng,Chin-Sien Moo,Yi-Ping Chen and Yao-Ching Hsieh, "Enhanced coulomb counting method for estimating state-of-charge and state-of-health of lithium-ion batteries," *Applied Energy,* pp. 1506-1511, 2009.

[31] Jun Xu and Binggang Cao, "Battery Management System for Electric Drive Vehicles – Modeling, State Estimation and Balancing," in *New Applications of Electric Drives*.

[32] "Wikipedia," [Online]. Available: https://en.wikipedia.org/wiki/Resistor.

[33] Hongwen He ,Rui Xiong and Jinxin Fan, "Evaluation of Lithium-Ion Battery Equivalent Circuit Models for State of Charge Estimation by an Experimental Approach," 2011.

[34] Haifeng Dai,Xuezhe Wei and Zechang Sun, "Recursive Parameter Identification of Lithium-Ion.Battery for EVs based on equivalent circuit model," *Journal of Computational and Theoretical Nanoscience,* 2013.

[35] Ahmad Rahmoun, Moritz Loske and Argo Rosin, "Determination of the Impedance of Lithium-Ion Batteries using," *Energy procedia,* 2013.

[36] J. Macdonald, Impedance spectroscopy, 1987.

[37] Jufeng Yang,Bing Xian,Yunlong Shang,Wenxin Huang and Chris Mi, "Improved Battery Parameter Estimation Method Considering Operating Scenarios for HEV/EV Applications," in *Advanced Energy Storage Technologies and Their Applications (AESA)*, 2016.

[38] Roberto Benato, "Sodium-nickel chloride (Na-NiCl2) battery safety tests for stationary electrochemical energy storage," 2016.

[39] Qingxia Yang, Jun Xu, Binggang Cao and Xiuqing Li, "A simplified fractional order impedance model and parameter identification method for lithium-ion batteries," 2017.

[40] C. H. Lim, "MIT OpenCourseWare," [Online]. Available: https://ocw.mit.edu/courses/chemical-engineering/10-626-electrochemical-energy-systems-spring-2014/lecture-notes/MIT10_626S14_S11lec20.pdf.

[41] "Research Solutions & Researches," [Online]. Available: http://www.consultrsr.net/resources/eis/cpe2.htm.

[42] "Electrochemistry resources," 2014. [Online]. Available: https://electrochemistryresources.com/the-constant-phase-element-cpe/.

[43] S.M.M. Alavi, C.R. Birkl, D.A. Howey, "Time-domain fitting of battery electrochemical impedance models," 2015.

[44] Bor Yann Liaw, Keith P. Bethune, and Chul Soo Kim , "Time-Series Field Trip Data Analysis Using Adaptive Recognition Approach. Analysis on Driving Patterns and Vehicle Usage for Electric Vehicles," 2002.

[45] Zhichao He, Geng Yang,and Languang Lu , "A Parameter Identification Method for Dynamics of Lithium Iron Phosphate Batteries Based on Step-Change Current Curves and Constant Current Curves," 2016.

[46] An Li, Serge Pelissier, Pascal Venet and Philippe Gyan, "Fast Characterization Method for Modeling Battery Relaxation Voltage," 2016.

[47] X. Hu, S. Li, H. Peng, and F. Sun, "Robustness analysis of state-of-charge estimation methods for two types of li-ion batteries," 2012.